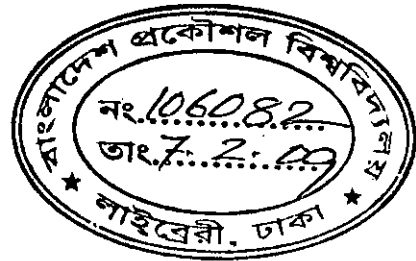


# SENSORLESS ADAPTIVE ROTOR PARAMETER ESTIMATION OF THREE PHASE INDUCTION MOTOR

A thesis submitted to the  
Department of Electrical and Electronic Engineering (EEE)  
of  
Bangladesh University of Engineering and Technology (BUET)  
in partial fulfillment of the requirements  
for the degree of  
MASTER OF SCIENCE IN ELECTRICAL AND ELECTRONIC ENGINEERING

By  
Rajib Mikail




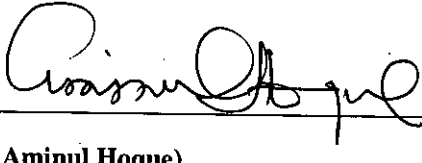
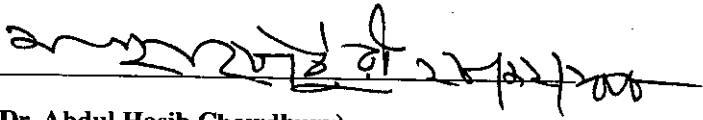

BUET



DEPARTMENT OF ELECTRICAL AND ELECTRONIC ENGINEERING (EEE)  
BANGLADESH UNIVERSITY OF ENGINEERING AND TECHNOLOGY (BUET)  
DHAKA - 1000, BANGLADESH  
DECEMBER 28, 2008


The thesis titled "SENSORLESS ADAPTIVE ROTOR PARAMETER ESTIMATION OF THREE PHASE INDUCTION MOTOR" submitted by Rajib Mikail, Roll No: 100606227P, Session: October 2006 has been accepted as satisfactory in partial fulfillment of the requirements for the degree of MASTER OF SCIENCE IN ELECTRICAL AND ELECTRONIC ENGINEERING on December 28, 2008.

### BOARD OF EXAMINERS

1.   
\_\_\_\_\_  
**(Dr. Kazi Mujibur Rahman)**  
Professor  
Department of EEE, BUET, Dhaka  
**Chairman**  
(Supervisor)
2.  28/12/08  
\_\_\_\_\_  
**(Dr. Aminul Hoque)**  
Professor and Head  
Department of EEE, BUET, Dhaka  
**Member**  
(Ex-officio)
3.   
\_\_\_\_\_  
**(Dr. Abdul Hasib Chowdhury)**  
Assistant Professor  
Department of EEE, BUET, Dhaka  
**Member**
4.   
\_\_\_\_\_  
**(Dr. M. Rezwana Khan)**  
Vice Chancellor  
United International University, Dhaka  
(Ex-Professor, EEE, BUET)  
**Member**  
(External)

# Declaration

The undersigned hereby declare that this thesis or any part of it has not been submitted elsewhere for the award of any degree or diploma.

 28.12.08

---

(Rajib Mikail)

Author

Dated: December 28, 2008

*To My Parents*

# Contents

<b>List of Tables</b>	<b>viii</b>
<b>List of Figures</b>	<b>ix</b>
<b>List of Symbols</b>	<b>xiii</b>
<b>Acknowledgements</b>	<b>xv</b>
<b>Abstract</b>	<b>xvi</b>
<b>1 Introduction</b>	<b>1</b>
1.1 Introduction	1
1.2 Objective	2
1.3 Scope of this Work	2
1.4 Review of Research in this Field	3
1.4.1 Field Oriented Control	3
1.4.2 Spectral Analysis Techniques	4
1.4.3 Observer Based Techniques	5
1.4.4 Model Reference Adaptive System Based Techniques	5
1.4.5 Fuzzy Logic Based Techniques	5
1.4.6 Artificial Neural Network Based Techniques	6
1.5 Outline of the Thesis	7
<b>2 Theory and modeling symmetrical Induction Machine</b>	<b>8</b>
2.1 Introduction	8
2.2 Equations in Machine Variables	8
2.3 Equations in Arbitrary Reference Frame Variables	13
2.4 Equations in Stationary Reference Frame Variables	18
2.5 Equations in Synchronously Rotating Reference Frame Variables	19
2.6 Equations in Rotor Reference Frame Variables	20

<b>3</b>	<b>Proposed Adaptation Scheme</b>	<b>22</b>
3.1	Matrix Formulations of the Model	22
3.2	The Adaptive Scheme	24
3.2.1	Sampling Step	26
3.2.2	The Change of Resistance Step	26
3.2.3	Runge-Kutta Solution Step	26
3.2.4	Current Magnitude Calculation Step	27
3.2.5	Rotor Resistance Update Step	27
3.2.6	Towards The Estimation Step	27
<b>4</b>	<b>Simulation Results</b>	<b>29</b>
4.1	Simulating the Model for 1hp Motor from Experimental Test Data	29
4.2	Simulating the Change of Rotor Resistance While Tracking the Change for the Test Data of an 1hp Motor	37
4.3	Simulating the Model for 3hp Motor	40
4.4	Simulating the Change of Rotor Resistance While Tracking the Change for the Test Data of a 3hp Motor	40
4.5	Simulating the Model for 5hp Motor	47
4.6	Simulating the Change of Rotor Resistance While Tracking the Change for the Test Data of a 5hp Motor	50
<b>5</b>	<b>Experimental Results</b>	<b>60</b>
5.1	The Test Data of an 1hp Motor	60
5.2	Hardware for Voltage Acquisition	60
5.3	Hardware for Current Acquisition	61
5.4	The Data Acquisition Card for Capturing Three Phase Voltages and Currents	63
5.5	The Adaptation Software Made by MATLAB GUIDE	64
<b>6</b>	<b>Conclusions and Future Works</b>	<b>68</b>
6.1	Conclusions of the Thesis	68
6.2	Future Works Proposed	69
	<b>References</b>	<b>70</b>

# List of Tables

Table 4.1	The test data for an 1hp motor	29
Table 4.2	The test data for a 3hp motor	40
Table 4.3	The test data for a 5hp motor	47
Table 5.1	Blocked rotor test data for an 1hp motor	60
Table 5.2	No load test data for an 1hp motor	61
Table 5.3	The parameters for an 1hp motor	61

# List of Figures

Figure 2.1	Equivalent Circuit Diagram (a) q- axis circuit (b) d- axis circuit (c) zero sequence circuit	13
Figure 3.1	Rotor resistance estimation by the adaptive scheme	25
Figure 4.1	The speed of an 1hp motor with the full load applied on 1.5s	30
Figure 4.2	The transient portion of the $d - q$ currents and the magnitude of the currents for an 1hp motor	31
Figure 4.3	The change of current magnitude while the full load is applied for an 1hp motor	31
Figure 4.4	The $d - q$ currents in synchronous reference frame while the full load is applied on 1.5 s for an 1hp motor	32
Figure 4.5	The $d - q$ currents in rotor reference frame while the full load is applied on 1.5 s for an 1hp motor	32
Figure 4.6	Transient and steady state portion of the torque while the full load is applied on 1.5s for an 1hp motor	33
Figure 4.7	The transient portion of the $d - q$ fluxes	33
Figure 4.8	The change of flux magnitude while the full load is applied for an 1hp motor	34
Figure 4.9	The $d - q$ fluxes in synchronous frame while the full load is applied on 1.5 s for an 1hp motor	34
Figure 4.10	The $d - q$ fluxes in rotor frame while the full load is applied on 1.5 s for an 1hp motor	35
Figure 4.11	The $d - q$ stator voltages in stator reference frame for an 1hp motor	35
Figure 4.12	The $d - q$ stator voltages in synchronous reference frame for an 1hp motor	36
Figure 4.13	The $d - q$ stator voltages in rotor reference frame for an 1hp motor	36
Figure 4.14	The torque is shown against speed for an 1hp motor	37



Figure 4.15	The change of current due to change of rotor resistance for an 1hp motor	38
Figure 4.16	The estimated rotor resistance is tracking the change made in the simulation for an 1hp motor	38
Figure 4.17	The percentage of error while tracking the change made in the simulation for an 1hp motor	39
Figure 4.18	The time to reach the original changed value while tracking the change made in the simulation for an 1hp motor	39
Figure 4.19	The speed of a 3hp motor with the full load applied on 1.5s	41
Figure 4.20	The change of current magnitude while the full load is applied for a 3hp motor	41
Figure 4.21	The $d - q$ currents in synchronous reference frame while the full load is applied on 1.5 s for a 3hp motor	42
Figure 4.22	The $d - q$ currents in rotor reference frame while the full load is applied on 1.5 s for a 3hp motor	42
Figure 4.23	Transient and steady state portion of the torque while the full load is applied on 1.5s for a 3hp motor	43
Figure 4.24	The transient portion of the $d - q$ fluxes	43
Figure 4.25	The change of flux magnitude while the full load is applied for a 3hp motor	44
Figure 4.26	The $d - q$ fluxes in synchronous frame while the full load is applied on 1.5 s for a 3hp motor	44
Figure 4.27	The $d - q$ fluxes in rotor frame while the full load is applied on 1.5 s for a 3hp motor	45
Figure 4.28	The $d - q$ stator voltages in stator reference frame for a 3hp motor	45
Figure 4.29	The $d - q$ stator voltages in synchronous reference frame for a 3hp motor	46
Figure 4.30	The $d - q$ stator voltages in rotor reference frame for a 3hp motor	46
Figure 4.31	The torque is shown against speed for a 3hp motor	47
Figure 4.32	The change of current due to change of rotor resistance for a 3hp motor	48
Figure 4.33	The estimated rotor resistance is tracking the change made in the simulation for a 3hp motor	48
Figure 4.34	The percentage of error while tracking the change made in the simulation for a 3hp motor	49

Figure 4.35	The time to reach the original changed value while tracking the change made in the simulation for a 3hp motor	49
Figure 4.36	The speed of a 5hp motor with the full load applied on 1.5s	50
Figure 4.37	The change of current magnitude while the full load is applied for a 5hp motor	51
Figure 4.38	The $d - q$ currents in synchronous reference frame while the full load is applied on 1.5 s for a 5hp motor	51
Figure 4.39	The $d - q$ currents in rotor reference frame while the full load is applied on 1.5 s for a 5hp motor	52
Figure 4.40	Transient and steady state portion of the while the full load is applied on 1.5s for a 5hp motor	52
Figure 4.41	The transient portion of the $d - q$ fluxes	53
Figure 4.42	The change of flux magnitude while the full load is applied for a 5hp motor	53
Figure 4.43	The $d - q$ fluxes in synchronous frame while the full load is applied on 1.5 s for a 5hp motor	54
Figure 4.44	The $d - q$ fluxes in rotor frame while the full load is applied on 1.5 s for a 5hp motor	54
Figure 4.45	The $d - q$ stator voltages in stator reference frame for a 5hp motor	55
Figure 4.46	The $d - q$ stator voltages in synchronous reference frame for a 5hp motor	55
Figure 4.47	The $d - q$ stator voltages in rotor reference frame for a 5hp motor	56
Figure 4.48	The torque is shown against speed for a 5hp motor	56
Figure 4.49	The change of current due to change of rotor resistance for a 5hp motor	57
Figure 4.50	The estimated rotor resistance is tracking the change made in the simulation for a 5hp motor	57
Figure 4.51	The percentage of error while tracking the change made in the simulation for a 5hp motor	58
Figure 4.52	The time to reach the original changed value while tracking the change made in the simulation for a 5hp motor	58
Figure 5.1	The switching inrush in the three phase voltages from the data acquisition card.	62

Figure 5.2	The switching inrush in the three phase currents from the data acquisition card.	63
Figure 5.3	The three phase voltages from the data acquisition card.	64
Figure 5.4	The three phase currents from the data acquisition card.	65
Figure 5.5	The experimentally captured and converted $d - q$ currents	65
Figure 5.6	The experimental setup of the whole system	66
Figure 5.7	The software window showing successful estimation of the rotor resistance	67
Figure 5.8	The software window showing successful estimation of the rotor resistance	67

# List of Symbols

$v_{as}$	Applied voltage of A phase in stator
$v_{bs}$	Applied voltage of B phase in stator
$v_{cs}$	Applied voltage of C phase in stator
$v_{ar}$	Applied voltage of A phase in rotor
$v_{br}$	Applied voltage of B phase in rotor
$v_{cr}$	Applied voltage of C phase in rotor
$i_{as}$	A phase stator current
$i_{bs}$	B phase stator current
$i_{cs}$	C phase stator current
$i_{ar}$	A phase rotor current
$i_{br}$	B phase rotor current
$i_{cr}$	C phase rotor current
$\psi_{as}$	Flux linkage in A phase of stator
$\psi_{bs}$	Flux linkage in B phase of stator
$\psi_{cs}$	Flux linkage in C phase of stator
$\psi_{ar}$	Flux linkage in A phase of rotor
$\psi_{br}$	Flux linkage in B phase of rotor
$\psi_{cr}$	Flux linkage in C phase of rotor
$R_s$	Stator per phase resistance
$R_r$	Rotor per phase resistance
$\psi_{abcs}$	Stator flux linkages in vector form
$\psi_{abcr}$	Rotor flux linkages in vector form
$\mathbf{L}_s$	Stator inductance matrix
$\mathbf{L}_r$	Rotor inductance matrix
$\mathbf{L}_{sr}$	Mutual inductance matrix
$L_{ls}$	Leakage inductance of the stator windings
$L_{lr}$	Leakage inductance of the rotor windings

$L_{ms}$	Magnetizing inductance of the stator windings
$L_{mr}$	Magnetizing inductance of the rotor windings
$L_{sr}$	Mutual inductance between stator and rotor
$N_s$	Stator equivalent turns
$N_r$	Rotor equivalent turns
$\mathbf{R}_s$	Stator resistance matrix
$\mathbf{R}_r$	Rotor resistance matrix
$\mathbf{R}'_r$	Rotor resistance matrix referred to stator
$\mathbf{f}_{abc}$	Three phase stator variables in vector form where $\mathbf{f}$ can represent either voltage, current, or flux linkage
$W_f$	Field energy
$W_c$	Coenergy
$T_e$	Electromagnetic output torque
$\theta_r$	Electrical angular displacement of rotor
$\theta_{rm}$	Actual angular displacement of the rotor
$P$	Number of poles in the machine
$\mathbf{f}_{dq0s}$	Direct axis and quadrature axis stator variables in vector form where $\mathbf{f}$ can represent either voltage, current, or flux linkage
$\mathbf{K}_s$	Reference frame conversion matrix for stator
$\mathbf{K}_r$	Reference frame conversion matrix for rotor
$\omega$	Angular velocity of the reference frame
$\omega_r$	Angular velocity of rotor
$L_m$	Mutual inductance in $d - q$ reference frame
$T_L$	Load Torque
$J$	Moment of inertia of the rotor
$B_r$	Frictional coefficient of the rotor
$\psi'_{dq0r}$	Rotor $d - q$ flux linkages in vector form referred to stator
$i'_{qr}$	Quadrature axis rotor current referred to stator in stator reference frame
$i'_{qr}$	Quadrature axis rotor current referred to stator in rotor reference frame
$i'_{qr}$	Quadrature axis rotor current referred to stator in synchronously rotating reference frame
$i'_{dr}$	Direct axis rotor current referred to stator in rotor reference frame

# Acknowledgements

First of all, I would like to express my heartfelt gratitude and very best regards to the Almighty Allah for making me successful in completing all the tasks.

I would like to thank Professor Dr. Kazi Mujibur Rahman, my supervisor, for his helpful suggestions and constant support during this research, without which this work could not be done.

I express my gratitude to Professor Dr. Mohammad Ali Choudhury for his positive influence, advice and inspiration to complete the research within two years.

I also express thank to Professor and Head, Dr. Aminul Hoque for his cooperation, suggestion and support.

Thanks to all my well wishers and friends who helped in various ways to complete the work.

BUET, Dhaka

December 28, 2008

Author

# Abstract

This thesis proposes, analyzes and verifies a sensorless adaptive rotor parameter estimation method for three phase induction motor. Accurate online parameter estimation is very important for inverter driven induction motor drives. Among the motor parameters the rotor is more prone to high percentage of parameter change. An adaptive rotor parameter estimation method is proposed including a detailed motor model. The motor model is simulated in different familiar reference frames. When the motor reaches steady state under constant load the stator current is monitored. The stator current of the motor is compared with the stator current of the model and the error is used recurrently to reestablish the model. The adaptation process stops when a threshold of the error value is reached. The estimated rotor resistance is compared with the original value. The response of the model is verified with different power rated motors. The responses with different change of parameters are also analyzed. An experimental setup is also arranged to verify the model.

# Chapter 1

## Introduction



### 1.1 Introduction

It is expected that computational power will lead to realization of more powerful control techniques in future. Adjustable speed AC drive technology gained a lot of momentum during the last few decades. AC motor drives consumes more than 60% of all electrical energy in industries. Induction motors, wound rotor synchronous motors and permanent magnet synchronous motors are the best candidates for variable speed drive applications. Though squirrel-cage induction motors are the cheapest, easy to maintain and manufactured up to several mega watts power ratings, the modeling and control strategy for such motors are complex compared to the other motors. Electromechanical drives are used for applications where the control of the position, speed, torque of the electric motor or the mechanical actuator is required. The early stages of research in motion control focussed on the application of basic control theory to drive a motor, using a power electronic converter. As the field evolved, it drew researchers from other fields, including control engineering, mechanical engineering, artificial intelligence, fuzzy logic, artificial neural networks and electrical machines. There are two central issues in control systems regarding AC drives. One is to make the resulting system of controller and plant robust against parameter variations and disturbances. The other is to make the system intelligent enough to make the system self adjusting to changes in environment and system parameters. Researchers are working in the drives area to find a computational effective, robust and intelligent control strategy. In the future, it is expected that computational power will lead to realization of more powerful control techniques. It will be possible to make a totally automatic control system. It will be possible to identify the required parameters, decide on the control strategy



and self-commission the drive.

## 1.2 Objective

The objective of this thesis is to propose, analyze and verify a sensorless adaptive rotor parameter estimation method for three phase induction motor. For inverter driven induction motor drives accurate online parameter estimation is very important. Among the motor parameters the rotor is more prone to high percentage of parameter change. A detailed motor model for the adaptive model is presented. The motor model is simulated in different familiar reference frames. The stator current of the motor is compared with the stator current of the model and the error is used recurrently to reestablish the model. The adaptation process stops when a threshold of the error value is reached. The response of the model is verified with different power rated motors. The responses with different change of parameters are also analyzed. For drives it is very crucial to accurately estimate or measure the changing parameters. If the estimated parameters are not accurate then the control signal and firing angle for the drives will go out of control. This work verifies a proposed adaptive scheme to estimate the rotor resistance within hardware in the loop control software.

## 1.3 Scope of this Work

In induction motor control drives, the major problem is variation in the rotor resistance which is affected by change in rotor temperature. The practical temperature excursion of the rotor is approximately 120°C above ambient. This increases the rotor resistances by 50 percent over its ambient or nominal value. When this parameter is incorrect in the controller, the calculated slip frequency is incorrect and the flux angle is no longer appropriate for field orientation. This results in instantaneous error in both flux and torque. Methods of overcoming this problem by a number of ways have been a major research goal for a number of years. The main objective of this thesis is to analyze, develop and implement a very fast on-line parameter identification algorithm using an adaptive model. Rotor parameter estimation of recent updates by Abdel et al [1] , Marcetic and Vukosavic [2] and Thongam et al [3] are all sensorless. Sensorless estimation is attracting the researchers as the reliability and durability of higher rated motors decreases if there is

any traditional torque sensors, speed sensors or flux sensors.

## **1.4 Review of Research in this Field**

The importance of tracking this rotor parameter and the methods of tracking developed up to date are reviewed hereafter.

### **1.4.1 Field Oriented Control**

In the area of induction motor drives the concept of Field Oriented Control (FOC) was introduced by Blaschke [4] in 1972. The armature and field fluxes are always perpendicular to each other in the dc motor. In an induction machine, a similar condition can be created with appropriate control of stator currents in the synchronously rotating frame of reference. FOC is a technique which provides a method of decoupling the two components of stator current, one producing the flux and the other producing the torque. Therefore it provides independent control of torque and flux during both dynamic and steady state conditions. The two basic schemes of field orientation are, Direct Field Oriented control (DFO) and Indirect Field Oriented control (IFO).

Direct Field Orientation originally proposed by Blaschke, requires flux acquisition which is mostly obtained from computational techniques using machine terminal quantities. Whereas IFO, proposed by Hasse, avoids the direct flux acquisition, by adding an estimated and regulated slip frequency to the shaft speed and integrating the total to obtain the stator flux position.

In DFO the position of the stator flux, which is essential for the correct orientation, is directly measured using search coils or estimated from terminal measurements. However using sensors to acquire the flux information, which needs installation of such sensors during machine manufacturing. Instead, the measured terminal quantities such as stator voltages and currents can be used. At very low frequencies the control becomes difficult. The indirect field oriented control method is essentially the same as direct field orientation, except that the flux position is generated in the feedforward manner. Indirect field orientation does not have inherent low speed problems and is thus preferred in most systems which must operate near zero speed.

In case of field oriented control the major problem is the rotor resistance which is sensitive to temperature. When this parameter is incorrect in the controller, the calculated slip frequency is incorrect and the flux angle is no longer appropriate for field orientation. This results in instantaneous error in both flux and torque. Both basic types of field orientation have sensitivity to machine parameters and provide non-ideal torque control characteristics when control parameters differ from the actual machine parameters. In general, both steady-state and dynamic responses of torque differ from the ideal instantaneous torque control achieved in theory by a correctly tuned controller.

### 1.4.2 Spectral Analysis Techniques

This method is based on the measured response to an injected test signal or an existing characteristic harmonic in the voltage/current spectrum. Stator currents and voltages of the motor are sampled and the parameters are derived from the spectral analysis of these samples. Matsuo and Lipo [5] proposed an on-line technique for determining the value of rotor resistance by detecting the negative sequence voltage. The main drawback of this method is that the strong harmonic torque pulsation is induced due to the interaction of positive and negative rotating components of MMF.

Toliyat and Hosseiny [6] presented another on-line estimation technique based on the d-q model in the frequency domain. The q-axis component of the injected negative sequence component is kept at zero, so that the motor torque is undisturbed. The d-axis component affects the motor flux. FFT is used to analyse the currents and voltages and the fundamental components of the sampled spectral values are used to determine the parameters. Average speed is used for the identification of parameters. Gabriel and Leonard [7] proposed a correlation method to detect misalignment between the actual motor flux and the rotor flux given by the model. A small auxiliary signal is added to the d-axis flux component of the stator current and a correlation function is evaluated.

Though rotor resistance can be estimated under any load and speed condition, the cost is high due to the installation of two search coils and will not be applicable to any off-the-shelf induction motor.

### **1.4.3 Observer Based Techniques**

Observer based techniques recently got momentum in this field. T. Matsuo and T. A. Lipo [5] proposed a method for detection of the inverse rotor time constant using the Extended Kalman Filter (EKF) by treating the rotor time constant as the fifth state variable along with the stator and rotor currents. B. K. Bose and N. R. Patel [8] also proposed EKF based control method. Here, the wide band harmonics contained in the PWM inverter output voltage serve as the perturbation. This method works on the assumption that when the motor speed changes, the machine model becomes a two input/two output time varying system with superimposed noise input. The drawbacks are that this method assumes that all other parameters are known and the magnetizing inductance can introduce large errors into the rotor time constant estimation. Finch et al. [9] proposed an application of EKF for slip calculation for tuning an IFO drive. Kubota et al. [10] proposed a DSP-based observer where the computational time is higher.

### **1.4.4 Model Reference Adaptive System Based Techniques**

Ohnishi et al [11] proposed a Model Reference Adaptive System against rotor resistance variation in 1986. This is the approach that has attracted most of the attention due to its relatively simple implementation requirements. Here the basic idea is to estimate certain states from two different directions, one is to calculate using states of the controllers and the other is to estimate the same states using measured signals. One of the estimates should be independent of rotor resistance, so that the error between these two estimates provide the correction to the rotor resistance, using an adaptive mechanism which can be a proportional-integral (PI) or integral controller. These methods essentially utilize the machine model and its accuracy is therefore heavily dependent on the accuracy of the model used. In general these methods primarily differ with respect to which quantity is selected for adaptation purposes. In this method rotor resistance adaptation is usually operational in steady-states only.

### **1.4.5 Fuzzy Logic Based Techniques**

Fuzzy logic based techniques are also used for the on-line rotor time constant / rotor resistance adaptation. In the fuzzy rotor resistance updating scheme proposed by Zidani et al [12], a direct estimate of the measured stator frequency is derived which is independent

of rotor resistance, and is taken as the measured stator frequency. The difference between these two measured and estimated was used to map the rotor resistance with a fuzzy logic function. In this paper they have activated the fuzzy estimator only in the steady-state.

Bim [13] proposed a fuzzy rotor time constant identification based on a fuzzy optimization problem in which the objective function is the total square error between the commanded stator currents and measured stator currents in the d-q reference frame. M. Ta-Cao and H. Le-Huy [14] estimated the rotor resistance, with only the steady-state measurements assuming the resistance variation is very slow.

#### **1.4.6 Artificial Neural Network Based Techniques**

Fodor et al. [15] investigated the possibility of using a neural network to compensate parameter variations in the IFO controlled induction motor drive. They added an off-line trained neural network as a black box, which estimates the time constant for the IFO controller. A rotor flux observer has been used to estimate the flux angle used for  $d - q$  transformation. The neural network was trained with a specific I/O pattern selected by the authors and only the steady-state model of the IFO controller was used. The major drawback of this type of learning is that the network may calculate the output with very large errors if the drive has to operate through an I/O pattern which was not investigated during the learning process.

Ba-Razzouk et al [16] proposed another ANN method for rotor time constant adaptation in IFO controlled drives. The training signals are generated with step variations in rotor resistance for different torque reference and flux command and the final network is connected in the IFO controller. The rotor time constant was tracked by a PI regulator that corrects any errors in the slip calculator. The output of this regulator is summed with that of the slip calculator and the result constitutes the new slip command that is required to compensate for the rotor time constant variation. The major drawback of this scheme is that the final neural network is only an off-line trained network with a limited data file in the modeling.

S. Mayaleh and N. Bayinder [17] proposed a rotor time constant estimation using a recurrent neural network. Their algorithm used the three stator voltage and three stator

current measurements in the stator reference frame.

## 1.5 Outline of the Thesis

The thesis begins with a review of induction rotor parameter estimation techniques in Chapter 1. The available literature covering on-line rotor time constant estimation techniques, broadly classified as spectral analysis techniques, observer based techniques, model reference adaptive system based techniques and the heuristic methods are reviewed in Chapter 1.

In Chapter 2, the detailed background theory of the whole work is presented. Here, at first the theory for a three phase symmetrical induction machine is presented. Then the theory for  $d - q$  reference frame is presented. For the reference frames the stationary, synchronously rotating reference frame, rotor reference frame are used. To convert the equations of different variables the arbitrary reference frame equations are presented.

In Chapter 3, the proposed adaptation process is presented. The theory of which is presented in the previous chapter. The whole adaptation scheme for rotor resistance estimation is presented step by step.

In Chapter 4, the simulation results for the model is presented. Simulation for different size of motors in respect of power capability is shown. Simulation for different reference models are also presented.

In Chapter 5, the experimental results are presented. The results of the adaptation process applied to a one horse power motor is investigated. The details of the experimental installation and data acquisition process is also presented.

Finally in Chapter 6, the conclusion and future works of the work is presented.

## Chapter 2

# Theory and modeling symmetrical Induction Machine

### 2.1 Introduction

To simulate the dynamic performance of typical symmetrical induction machines and to depict the variables in various reference frames during acceleration and deceleration periods, details theory and modeling of the machine is necessary. In this chapter the detailed voltage and torque equations in terms of machine variables are presented [18]-[19]. Transformation to arbitrary reference frame accommodating rotating circuits is also presented. Once the arbitrary reference frame equations are established the equations may then be expressed in any reference frame with exact assignment of the speed of the reference frame. Although the stationary reference frame, the rotor reference frame and synchronous reference frame are most frequently used, the arbitrary reference frame offers a direct means of obtaining the voltage equations in these and all other reference frames.

### 2.2 Equations in Machine Variables

The three stator windings are considered identical, sinusoidally distributed and  $120^\circ$  displaced with  $N_s$  equivalent turns and resistance  $R_s$ . The three rotor windings are also considered as identical, sinusoidally distributed, displaced  $120^\circ$ , with  $N_r$  equivalent turns and resistance  $R_r$ . The stator and rotor  $a - b - c$  phase voltage equations in machine variables are expressed as

$$\begin{bmatrix} v_{as} \\ v_{bs} \\ v_{cs} \end{bmatrix} = \begin{bmatrix} R_s & 0 & 0 \\ 0 & R_s & 0 \\ 0 & 0 & R_s \end{bmatrix} \begin{bmatrix} i_{as} \\ i_{bs} \\ i_{cs} \end{bmatrix} + \frac{d}{dt} \begin{bmatrix} \psi_{as} \\ \psi_{bs} \\ \psi_{cs} \end{bmatrix} \quad (2.1)$$

$$\begin{bmatrix} v_{ar} \\ v_{br} \\ v_{cr} \end{bmatrix} = \begin{bmatrix} R_r & 0 & 0 \\ 0 & R_r & 0 \\ 0 & 0 & R_r \end{bmatrix} \begin{bmatrix} i_{ar} \\ i_{br} \\ i_{cr} \end{bmatrix} + \frac{d}{dt} \begin{bmatrix} \psi_{ar} \\ \psi_{br} \\ \psi_{cr} \end{bmatrix} \quad (2.2)$$

The  $s$  subscript denotes variables and parameters associated with stator circuits, and the  $r$  subscript denotes variables and parameters associated with rotor circuits. For a magnetically linear system, the flux linkages are expressed as

$$\begin{bmatrix} \psi_{abcs} \\ \psi_{abcr} \end{bmatrix} = \begin{bmatrix} \mathbf{L}_s & \mathbf{L}_{sr} \\ (\mathbf{L}_{sr})^T & \mathbf{L}_r \end{bmatrix} \begin{bmatrix} \mathbf{i}_{abcs} \\ \mathbf{i}_{abcr} \end{bmatrix} \quad (2.3)$$

where,

$$(\mathbf{f}_{abcs})^T = [f_{as} \quad f_{bs} \quad f_{cs}] \quad (2.4)$$

$$(\mathbf{f}_{abcr})^T = [f_{ar} \quad f_{br} \quad f_{cr}] \quad (2.5)$$

$f$  can represent either voltage, current, or flux linkage.

$$\mathbf{L}_s = \begin{bmatrix} L_{ls} + L_{ms} & -\frac{1}{2}L_{ms} & -\frac{1}{2}L_{ms} \\ -\frac{1}{2}L_{ms} & L_{ls} + L_{ms} & -\frac{1}{2}L_{ms} \\ -\frac{1}{2}L_{ms} & -\frac{1}{2}L_{ms} & L_{ls} + L_{ms} \end{bmatrix} \quad (2.6)$$

$$\mathbf{L}_r = \begin{bmatrix} L_{lr} + L_{mr} & -\frac{1}{2}L_{mr} & -\frac{1}{2}L_{mr} \\ -\frac{1}{2}L_{mr} & L_{lr} + L_{mr} & -\frac{1}{2}L_{mr} \\ -\frac{1}{2}L_{mr} & -\frac{1}{2}L_{mr} & L_{lr} + L_{mr} \end{bmatrix} \quad (2.7)$$

$$\mathbf{L}_{sr} = L_{sr} \begin{bmatrix} \cos \theta_r & \cos(\theta_r + 120^\circ) & \cos(\theta_r - 120^\circ) \\ \cos(\theta_r - 120^\circ) & \cos \theta_r & \cos(\theta_r + 120^\circ) \\ \cos(\theta_r + 120^\circ) & \cos(\theta_r - 120^\circ) & \cos \theta_r \end{bmatrix} \quad (2.8)$$



In the above inductance equations  $L_{ls}$  and  $L_{ms}$  are respectively the leakage and magnetizing inductances of the stator windings.  $L_{lr}$  and  $L_{mr}$  are for the rotor windings.  $L_{sr}$  is the mutual inductances between stator and rotor windings.

For the machine rotor which has uniformly distributed skewed copper or aluminum bars embedded in a ferromagnetic material with all bars terminated in a common ring at each end of the rotor, are referred to as squirrel cage rotor. This configuration is equivalent to uniformly and sinusoidally distributed three phase windings as stator.

It is convenient to refer all rotor variables to the stator windings by appropriate turns ratios.

$$\mathbf{i}'_{abcr} = \frac{N_r}{N_s} \mathbf{i}_{abcr} \quad (2.9)$$

$$\mathbf{v}'_{abcr} = \frac{N_s}{N_r} \mathbf{v}_{abcr} \quad (2.10)$$

$$\Psi'_{abcr} = \frac{N_s}{N_r} \Psi_{abcr} \quad (2.11)$$

The magnetizing and mutual inductances are associated with the same magnetic flux path. Therefore,

$$L_{ms} = \frac{N_s}{N_r} L_{sr} \quad (2.12)$$

and

$$L_{sr} = \frac{N_s}{N_r} L_{mr} \quad (2.13)$$

So, we can get,

$$L_{ms} = \left( \frac{N_s}{N_r} \right)^2 L_{mr} \quad (2.14)$$

Thus,

$$\mathbf{L}'_{sr} = \frac{N_s}{N_r} \mathbf{L}_{sr} = L_{ms} \begin{bmatrix} \cos \theta_r & \cos(\theta_r + 120^\circ) & \cos(\theta_r - 120^\circ) \\ \cos(\theta_r - 120^\circ) & \cos \theta_r & \cos(\theta_r + 120^\circ) \\ \cos(\theta_r + 120^\circ) & \cos(\theta_r - 120^\circ) & \cos \theta_r \end{bmatrix} \quad (2.15)$$

Also,  $L_{mr}$  is expressed as

$$L_{mr} = \left( \frac{N_r}{N_s} \right)^2 L_{sr} \quad (2.16)$$

and

$$\mathbf{L}'_r = \left( \frac{N_s}{N_r} \right)^2 \mathbf{L}_r \quad (2.17)$$

from (2.7),  $\mathbf{L}'_r$  can be expressed as

$$\mathbf{L}'_r = \begin{bmatrix} L'_{lr} + L_{mr} & -\frac{1}{2}L_{mr} & -\frac{1}{2}L_{mr} \\ -\frac{1}{2}L_{mr} & L'_{lr} + L_{mr} & -\frac{1}{2}L_{mr} \\ -\frac{1}{2}L_{mr} & -\frac{1}{2}L_{mr} & L'_{lr} + L_{mr} \end{bmatrix} \quad (2.18)$$

where,

$$L'_{lr} = \left( \frac{N_s}{N_r} \right)^2 L_{lr} \quad (2.19)$$

The flux linkages can be expressed as

$$\begin{bmatrix} \psi_{abcs} \\ \psi'_{abcr} \end{bmatrix} = \begin{bmatrix} \mathbf{L}_s & \mathbf{L}'_{sr} \\ (\mathbf{L}'_{sr})^T & \mathbf{L}'_r \end{bmatrix} \begin{bmatrix} \mathbf{i}_{abcs} \\ \mathbf{i}'_{abcr} \end{bmatrix} \quad (2.20)$$

The voltage equations expressed in terms of machine variables referred to the stator windings are

$$\begin{bmatrix} \mathbf{v}_{abcs} \\ \mathbf{v}'_{abcr} \end{bmatrix} = \begin{bmatrix} \mathbf{R}_s + \frac{d}{dt} \mathbf{L}_s & \frac{d}{dt} \mathbf{L}'_{sr} \\ \frac{d}{dt} (\mathbf{L}'_{sr})^T & \mathbf{R}'_r + \frac{d}{dt} \mathbf{L}'_r \end{bmatrix} \begin{bmatrix} \mathbf{i}_{abcs} \\ \mathbf{i}'_{abcr} \end{bmatrix} \quad (2.21)$$

where  $\mathbf{R}_s, \mathbf{R}_r$  are diagonal matrices and

$$\mathbf{R}'_r = \left( \frac{N_s}{N_r} \right)^2 \mathbf{R}_r \quad (2.22)$$

The energy stored in a magnetically linear system is the sum of the self inductance of each winding times one-half the square of its current and all mutual inductances, each times the currents in the two windings coupled by the mutual inductance. The energy stored in the leakage inductances is not a part of the energy stored in the coupling field. Therefore the energy stored in the coupling field is written as

$$W_f = \frac{1}{2} (\mathbf{i}_{abcs})^T (\mathbf{L}_s - L_{ls} \mathbf{I}) \mathbf{i}_{abcs} + (\mathbf{i}_{abcs})^T \mathbf{L}_{sr} \mathbf{i}'_{abcr} + \frac{1}{2} (\mathbf{i}'_{abcr})^T (\mathbf{L}'_r - L'_{lr} \mathbf{I}) \mathbf{i}'_{abcr} \quad (2.23)$$

Where  $\mathbf{I}$  is the identity matrix. Since the machine is assumed to be magnetically linear the field energy  $W_f$  is equal to the coenergy  $W_c$ .

In a rotational system the change of mechanical energy can be represented as

$$dW_m = -T_e d\theta_{rm} \quad (2.24)$$

where  $T_e$  is the electromagnetic output torque and  $\theta_{rm}$  is the actual angular displacement of the rotor. The electrical angular displacement  $\theta_r$  is

$$\theta_r = \left( \frac{P}{2} \right) \theta_{rm} \quad (2.25)$$

where  $P$  is the number of poles in the machine, then

$$dW_m = -T_e \left( \frac{2}{P} \right) d\theta_{rm} \quad (2.26)$$

Since  $W_f = W_c$ , the electromagnetic torque may be evaluated as

$$T_e(i_j, \theta_r) = \left( \frac{P}{2} \right) \frac{\partial W_c(i_j, \theta_r)}{\partial \theta_r} \quad (2.27)$$

As  $\mathbf{L}_s$  and  $\mathbf{L}'_r$  are not functions of  $\theta_r$ , the electromagnetic developed torque can be expressed as

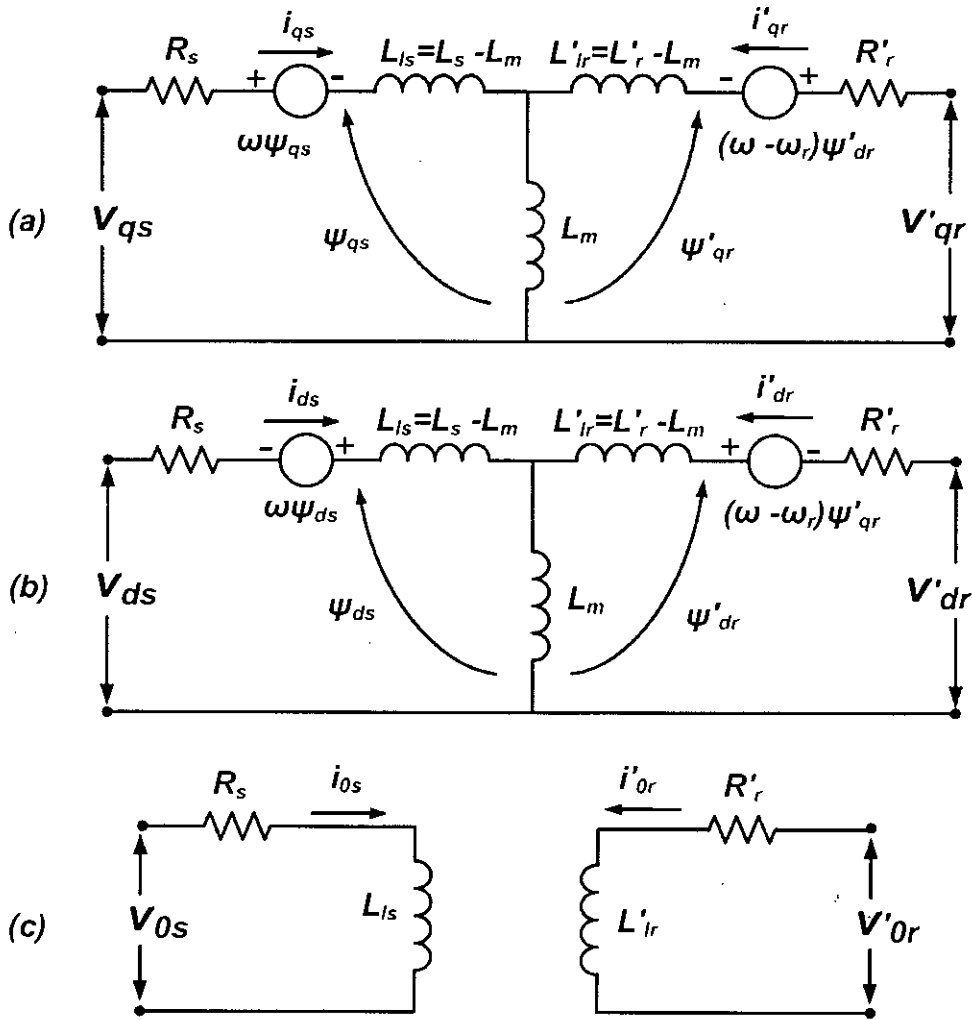


Figure 2.1: Equivalent Circuit Diagram (a) q- axis circuit (b) d- axis circuit (c) zero sequence circuit

$$T_e = \left(\frac{P}{2}\right) (\mathbf{i}_{abcs})^T \frac{\partial}{\partial \theta_r} [\mathbf{L}'_{sr}] \mathbf{i}'_{abcr} \quad (2.28)$$

### 2.3 Equations in Arbitrary Reference Frame Variables

The three phase reference frame variables can be transformed to two phase reference frame variables. The corresponding equivalent circuit for the machine is shown in Figure 2.1 .

The relationship for stator is as follows

$$\mathbf{f}_{qd0s} = \mathbf{K}_s \mathbf{f}_{abcs} \quad (2.29)$$

where,

$$\mathbf{K}_s = \begin{bmatrix} \cos \theta & \cos(\theta - 120^\circ) & \cos(\theta + 120^\circ) \\ \sin \theta & \sin(\theta - 120^\circ) & \sin(\theta + 120^\circ) \\ 0.5 & 0.5 & 0.5 \end{bmatrix} \quad (2.30)$$

and

$$\theta = \int_0^t \omega(\xi) d\xi + \theta(0) \quad (2.31)$$

The relationship for rotor is as follows,

$$\mathbf{f}_{qd0r} = \mathbf{K}_r \mathbf{f}_{abcr} \quad (2.32)$$

where

$$\mathbf{K}_r = \begin{bmatrix} \cos(\theta - \theta_r) & \cos(\theta - \theta_r - 120^\circ) & \cos(\theta - \theta_r + 120^\circ) \\ \sin(\theta - \theta_r) & \sin(\theta - \theta_r - 120^\circ) & \sin(\theta - \theta_r + 120^\circ) \\ 0.5 & 0.5 & 0.5 \end{bmatrix} \quad (2.33)$$

and

$$\theta_r = \int_0^t \omega_r(\xi) d\xi + \theta_r(0) \quad (2.34)$$

In the above equations,  $f_q$  is the quadrature axis component,  $f_d$  is the direct axis component and  $f_0$  is the zero sequence component,  $f$  can represent either voltage, current, or flux linkage. The angular velocity of the new reference frame with respect to stationary stator is  $\omega$  and it may be constant, varying, or zero. The angular velocity of rotor with respect to stationary stator is  $\omega_r$ .

Equation 2.1 can be written in  $d - q$  reference frame as

$$\begin{aligned}
v_{qd0s} &= \mathbf{K}_s(\mathbf{R}_s \mathbf{i}_{abcs} + \frac{d}{dt} \psi_{abcs}) \\
&= \mathbf{K}_s(\mathbf{R}_s \mathbf{i}_{abcs}) + \mathbf{K}_s(\frac{d}{dt} \psi_{abcs}) \\
&= \mathbf{K}_s \mathbf{R}_s (\mathbf{K}_s)^{-1} \mathbf{i}_{qd0s} + \mathbf{K}_s \frac{d}{dt} [(\mathbf{K}_s)^{-1} \psi_{qd0s}] \\
&= \mathbf{R}_s \mathbf{i}_{qd0s} + \mathbf{K}_s \frac{d}{dt} [(\mathbf{K}_s)^{-1}] \psi_{qd0s} + \mathbf{K}_s (\mathbf{K}_s)^{-1} \frac{d}{dt} \psi_{qd0s} \\
&= \mathbf{R}_s \mathbf{i}_{qd0s} + \omega \psi_{dqs} + \frac{d}{dt} \psi_{qd0s}
\end{aligned} \tag{2.35}$$

where,

$$\mathbf{K}_s \frac{d}{dt} [(\mathbf{K}_s)^{-1}] = \omega \begin{bmatrix} 0 & 1 & 0 \\ -1 & 0 & 0 \\ 0 & 0 & 0 \end{bmatrix} \tag{2.36}$$

and

$$\psi_{dqs} = \begin{bmatrix} \psi_{ds} \\ -\psi_{qs} \\ 0 \end{bmatrix} \tag{2.37}$$

From the above equations the expanded forms of the variables, for both stator and by similar derivation for rotor referred to stator, can be shown that

$$v_{qs} = R_s i_{qs} + \omega \psi_{ds} + \frac{d}{dt} \psi_{qs} \tag{2.38}$$

$$v_{ds} = R_s i_{ds} - \omega \psi_{qs} + \frac{d}{dt} \psi_{ds} \tag{2.39}$$

$$v_{0s} = R_s i_{0s} + \frac{d}{dt} \psi_{0s} \tag{2.40}$$

$$v'_{qr} = R'_r i'_{qr} + (\omega - \omega_r) \psi'_{dr} + \frac{d}{dt} \psi'_{qr} \tag{2.41}$$

$$v'_{dr} = R'_r i'_{dr} - (\omega - \omega_r) \psi'_{qr} + \frac{d}{dt} \psi'_{dr} \quad (2.42)$$

$$v'_{0r} = R'_r i'_{0r} + \frac{d}{dt} \psi'_{0r} \quad (2.43)$$

In  $d - q$  frame the flux linkage equations can shown from 2.20 as

$$\begin{bmatrix} \psi_{qd0s} \\ \psi'_{qd0r} \end{bmatrix} = \begin{bmatrix} \mathbf{K}_s \mathbf{L}_s (\mathbf{K}_s)^{-1} & \mathbf{K}_s \mathbf{L}'_{sr} (\mathbf{K}_r)^{-1} \\ \mathbf{K}_s (\mathbf{L}'_{sr})^T (\mathbf{K}_s)^{-1} & \mathbf{K}_r \mathbf{L}'_{r} (\mathbf{K}_r)^{-1} \end{bmatrix} \begin{bmatrix} \mathbf{i}_{qd0s} \\ \mathbf{i}'_{qd0r} \end{bmatrix} \quad (2.44)$$

From 2.6 it can be shown that

$$\mathbf{K}_s \mathbf{L}_s (\mathbf{K}_s)^{-1} = \begin{bmatrix} L_{ls} + L_m & 0 & 0 \\ 0 & L_{ls} + L_m & 0 \\ 0 & 0 & L_{ls} \end{bmatrix} \quad (2.45)$$

where,  $L_m = 3/2 L_{ms}$

From 2.7 it can be shown that

$$\mathbf{K}_r \mathbf{L}'_{r} (\mathbf{K}_r)^{-1} = \begin{bmatrix} L'_{lr} + L_m & 0 & 0 \\ 0 & L'_{lr} + L_m & 0 \\ 0 & 0 & L'_{lr} \end{bmatrix} \quad (2.46)$$

From 2.8 it can be shown that

$$\mathbf{K}_s \mathbf{L}'_{sr} (\mathbf{K}_r)^{-1} = \mathbf{K}_s (\mathbf{L}'_{sr})^T (\mathbf{K}_s)^{-1} = \begin{bmatrix} L_m & 0 & 0 \\ 0 & L_m & 0 \\ 0 & 0 & 0 \end{bmatrix} \quad (2.47)$$

So, the expanded expressions for the flux linkages are

$$\psi_{qs} = L_{ls} i_{qs} + L_m (i_{qs} + i'_{qr}) \quad (2.48)$$

$$\psi_{ds} = L_{ls} i_{ds} + L_m (i_{ds} + i'_{dr}) \quad (2.49)$$

$$\Psi_{0s} = L_{ls}i_{0s} \quad (2.50)$$

$$\Psi'_{qr} = L'_{ls}i'_{qr} + L_m(i_{qs} + i'_{qr}) \quad (2.51)$$

$$\Psi'_{dr} = L'_{ls}i'_{dr} + L_m(i_{ds} + i'_{dr}) \quad (2.52)$$

$$\Psi'_{0r} = L'_{ls}i'_{0r} \quad (2.53)$$

The electromagnetic torque in terms of  $d - q$  reference frame variables is found from 2.28 as

$$T_e = \left(\frac{P}{2}\right) \left[ (\mathbf{K}_s)^{-1} \mathbf{i}_{qd0s} \right]^T \frac{\partial}{\partial \theta_r} \left[ \mathbf{L}'_{sr} \right] (\mathbf{K}_r)^{-1} \mathbf{i}'_{qd0r} \quad (2.54)$$

In terms of currents the expression is found as

$$T_e = \left(\frac{3}{2}\right) \left(\frac{P}{2}\right) L_m (i_{qs}i'_{dr} - i_{ds}i'_{qr}) \quad (2.55)$$

Which can also be written in other machine variables as

$$T_e = \left(\frac{3}{2}\right) \left(\frac{P}{2}\right) (\Psi'_{qr}i'_{dr} - \Psi'_{dr}i'_{qr}) \quad (2.56)$$

$$T_e = \left(\frac{3}{2}\right) \left(\frac{P}{2}\right) (\Psi_{ds}i_{qs} - \Psi_{qs}i_{ds}) \quad (2.57)$$

The angular speed is related to the torque as

$$T_e = T_L + J \frac{d\omega_m}{dt} + B_r \omega_m \quad (2.58)$$

$$T_e = T_L + \frac{2}{P} (J \frac{d\omega_r}{dt} + B_r \omega_r) \quad (2.59)$$

where,  $\omega_m$  is the rotor mechanical speed and  $\omega_r$  is the rotor electrical speed,  $J$  is the moment of inertia of the rotor,  $B_r$  is the frictional coefficient.



## 2.4 Equations in Stationary Reference Frame Variables

The dynamic machine model can be obtained by substituting  $\omega = 0$  in the above equations. The corresponding stationary frame voltage equations for a singly fed machine are as follows

$$v_{qs}^s = R_s i_{qs}^s + \frac{d}{dt} \psi_{qs}^s \quad (2.60)$$

$$v_{ds}^s = R_s i_{ds}^s + \frac{d}{dt} \psi_{ds}^s \quad (2.61)$$

$$v_{0s}^s = R_s i_{0s}^s + \frac{d}{dt} \psi_{0s}^s \quad (2.62)$$

$$0 = R_r' i_{qr}'^s - \omega_r \psi_{dr}'^s + \frac{d}{dt} \psi_{qr}'^s \quad (2.63)$$

$$0 = R_r' i_{dr}'^s + \omega_r \psi_{qr}'^s + \frac{d}{dt} \psi_{dr}'^s \quad (2.64)$$

$$0 = R_r' i_{0r}'^s + \frac{d}{dt} \psi_{0r}'^s \quad (2.65)$$

The  $s$  superscript is for the indication of stationary reference frame. The corresponding stationary frame torque equations are

$$T_e = \left(\frac{3}{2}\right) \left(\frac{P}{2}\right) L_m (i_{qs}^s i_{dr}'^s - i_{ds}^s i_{qr}'^s) \quad (2.66)$$

$$T_e = \left(\frac{3}{2}\right) \left(\frac{P}{2}\right) (\psi_{qr}'^s i_{dr}'^s - \psi_{dr}'^s i_{qr}'^s) \quad (2.67)$$

$$T_e = \left(\frac{3}{2}\right) \left(\frac{P}{2}\right) (\psi_{ds}^s i_{qs}^s - \psi_{qs}^s i_{ds}^s) \quad (2.68)$$

## 2.5 Equations in Synchronously Rotating Reference Frame Variables

The dynamic machine model can be obtained by substituting  $\omega = \omega_e$  in the above equations. The corresponding synchronously rotating reference frame voltage equations for a singly fed machine are as follows

$$v_{qs}^e = R_s i_{qs}^e + \omega_e \psi_{ds}^e + \frac{d}{dt} \psi_{qs}^e \quad (2.69)$$

$$v_{ds}^e = R_s i_{ds}^e - \omega_e \psi_{qs}^e + \frac{d}{dt} \psi_{ds}^e \quad (2.70)$$

$$v_{0s}^e = R_s i_{0s}^e + \frac{d}{dt} \psi_{0s}^e \quad (2.71)$$

$$0 = R_r' i_{qr}^e + (\omega_e - \omega_r) \psi_{dr}^e + \frac{d}{dt} \psi_{qr}^e \quad (2.72)$$

$$0 = R_r' i_{dr}^e - (\omega_e - \omega_r) \psi_{qr}^e + \frac{d}{dt} \psi_{dr}^e \quad (2.73)$$

$$0 = R_r' i_{0r}^e + \frac{d}{dt} \psi_{0r}^e \quad (2.74)$$

The  $e$  superscript is for the indication of synchronously rotating reference frame. The corresponding synchronously rotating reference frame torque equations are

$$T_e = \left(\frac{3}{2}\right) \left(\frac{P}{2}\right) L_m (i_{qs}^e i_{dr}^e - i_{ds}^e i_{qr}^e) \quad (2.75)$$

$$T_e = \left(\frac{3}{2}\right) \left(\frac{P}{2}\right) (\psi_{qr}^e i_{dr}^e - \psi_{dr}^e i_{qr}^e) \quad (2.76)$$

$$T_e = \left(\frac{3}{2}\right) \left(\frac{P}{2}\right) (\psi_{ds}^e i_{qs}^e - \psi_{qs}^e i_{ds}^e) \quad (2.77)$$

## 2.6 Equations in Rotor Reference Frame Variables

The dynamic machine model can be obtained by substituting  $\omega = \omega_r$  in the above equations. The corresponding rotor reference frame voltage equations for a singly fed machine are as follows

$$v_{qs}^r = R_s i_{qs}^r + \omega_r \psi_{ds}^r + \frac{d}{dt} \psi_{qs}^r \quad (2.78)$$

$$v_{ds}^r = R_s i_{ds}^r - \omega_r \psi_{qs}^r + \frac{d}{dt} \psi_{ds}^r \quad (2.79)$$

$$v_{0s}^r = R_s i_{0r}^r + \frac{d}{dt} \psi_{0s}^r \quad (2.80)$$

$$0 = R_r i_{qr}^r + \frac{d}{dt} \psi_{qr}^r \quad (2.81)$$

$$0 = R_r i_{dr}^r + \frac{d}{dt} \psi_{dr}^r \quad (2.82)$$

$$0 = R_r i_{0r}^r + \frac{d}{dt} \psi_{0r}^r \quad (2.83)$$

The  $r$  superscript is for the indication of rotor reference frame. The corresponding rotor reference frame torque equations are

$$T_e = \left(\frac{3}{2}\right) \left(\frac{P}{2}\right) L_m (i_{qs}^r i_{dr}^r - i_{ds}^r i_{qr}^r) \quad (2.84)$$

$$T_e = \left(\frac{3}{2}\right) \left(\frac{P}{2}\right) (\psi_{qr}^r i_{dr}^r - \psi_{dr}^r i_{qr}^r) \quad (2.85)$$

$$T_e = \left(\frac{3}{2}\right) \left(\frac{P}{2}\right) (\psi_{ds}^r i_{qs}^r - \psi_{qs}^r i_{ds}^r) \quad (2.86)$$

The detailed background theory of the whole work is presented. Here, at first the theory for a three phase symmetrical induction machine is presented. Then the theory for  $d - q$  reference frame is presented. To convert the equations of different variables the arbitrary reference frame equations are presented. For the reference frames the stationary, synchronously rotating reference frame, rotor reference frames are used. The theory presented here is the basis of the adaptive model presented in Chapter 3. The arbitrary reference frame equations are used to establish the state space model equations for the proposed adaptation scheme.

# Chapter 3

## Proposed Adaptation Scheme

The detail theory for the adaptive model is presented in the previous chapter. The proposed adaptation process is presented. The theory of which is presented in the previous chapter. The whole adaptation scheme for rotor resistance estimation is presented step by step. The model proposed here is solved by Runge-Kutta method to find the various stator and rotor parameters during the simulation. The simulation is done by MATLAB. A model block diagram is presented to illustrate the whole scheme.

### 3.1 Matrix Formulations of the Model

To illustrate the adaptation process we need to rewrite the  $d - q$  reference frame model equations of (2.38) to (2.43) in matrix formulations as :

$$\mathbf{V} = \mathbf{R}\mathbf{I} + \mathbf{W}\mathbf{L}\mathbf{I} + \mathbf{L}\frac{d\mathbf{I}}{dt} \quad (3.1)$$

where,

$$\mathbf{V} = \begin{bmatrix} v_{ds} \\ v_{qs} \\ 0 \\ 0 \end{bmatrix} \quad \mathbf{R} = \begin{bmatrix} R_s & 0 & 0 & 0 \\ 0 & R_s & 0 & 0 \\ 0 & 0 & R'_r & 0 \\ 0 & 0 & 0 & R'_r \end{bmatrix} \quad \mathbf{I} = \begin{bmatrix} i_{ds} \\ i_{qs} \\ i'_{dr} \\ i'_{qr} \end{bmatrix}$$

$$\mathbf{L} = \begin{bmatrix} L_{sl} + L_m & 0 & L_m & 0 \\ 0 & L_{sl} + L_m & 0 & L_m \\ L_m & 0 & L'_{rl} + L_m & 0 \\ 0 & L_m & 0 & L'_{rl} + L_m \end{bmatrix}$$

$$\mathbf{W} = \begin{bmatrix} 0 & -\omega & 0 & 0 \\ \omega & 0 & 0 & 0 \\ 0 & 0 & 0 & -(\omega - \omega_m) \\ 0 & 0 & (\omega - \omega_m) & 0 \end{bmatrix}$$

The flux linkages for  $d - q$  reference frame is calculated from

$$\psi = \mathbf{L}\mathbf{I} \quad (3.2)$$

where,

$$\psi = \begin{bmatrix} \psi_{ds} \\ \psi_{qs} \\ \psi_{dr} \\ \psi_{qr} \end{bmatrix}$$

The torque equations used for state space solution is

$$T_e = \left(\frac{3}{2}\right) \left(\frac{P}{2}\right) L_m (i_{qs}i'_{dr} - i_{ds}i'_{qr}) \quad (3.3)$$

$$\frac{d\omega_m}{dt} = (T_e - T_L)/J - B_r\omega_m/J \quad (3.4)$$

Where,  $\omega_m$  is the rotor mechanical speed. For state space solution the angle is also a output variable and it is given in the model as,

$$\frac{d\theta_m}{dt} = \omega_m \quad (3.5)$$

## 3.2 The Adaptive Scheme

The three phase voltages are captured to the computer through data acquisition card. To capture the three phase voltages to the computer the three phase supply needs to be stepped down. Three 220V – 12V, 5A transformers were bought for this purpose. The three transformers were *Y* connected in the primary side. The neutral of that *Y* connection was connected to the neutral of the motor *Y* connection. The output of the three transformers were further stepped down through resistance voltage divider to restrict the voltage provided to the data acquisition card to comply with the input limit of the card. As the maximum input limit of the card channels is 10V. The resistance voltage divider was set to 5 by 1 so that the maximum voltage that may occur across the channels should not go beyond the limit even when an inrush voltage comes at the moment of switching off the motor.

The value of three phase currents were passed to the data acquisition card through current transformers. The primary vs secondary turns ratio is 300 by 5. The outputs of the current transformers were shorted by three 0.5 $\Omega$  each. This time also the voltage across the 0.5 $\Omega$  is within the limit of the data acquisition card. The inrush current while switching on the motor is higher than the steady state current.

The data acquisition card used here is PCI-1711L of Advantech Corporation. It has 16 analog input channels. The maximum sampling rate of the card per channel is 100 kilo sample per second. For the hardware in the loop simulation 10 kilo sample per second per channel were used. Because if the sampling rate is higher then necessary the estimation process calculation increases. The three phase voltages and currents sampled to the computer were calibrated. For calibration purpose of the voltages the multiplying factor were calculated by dividing the measured the input voltages to the transformers by a high precision multimeter by the sampled voltages from the data acquisition card. For the calibration of the currents measured by the data acquisition card the three phase currents were also measured by high precision current meters and the proper multiplying factors were calculated as well. The detail adaptation process is explained in Figure 3.1.

The algorithm of the adaptive scheme is explained in step by step as:

**Step1** : Start capturing currents from motor three phase lines.

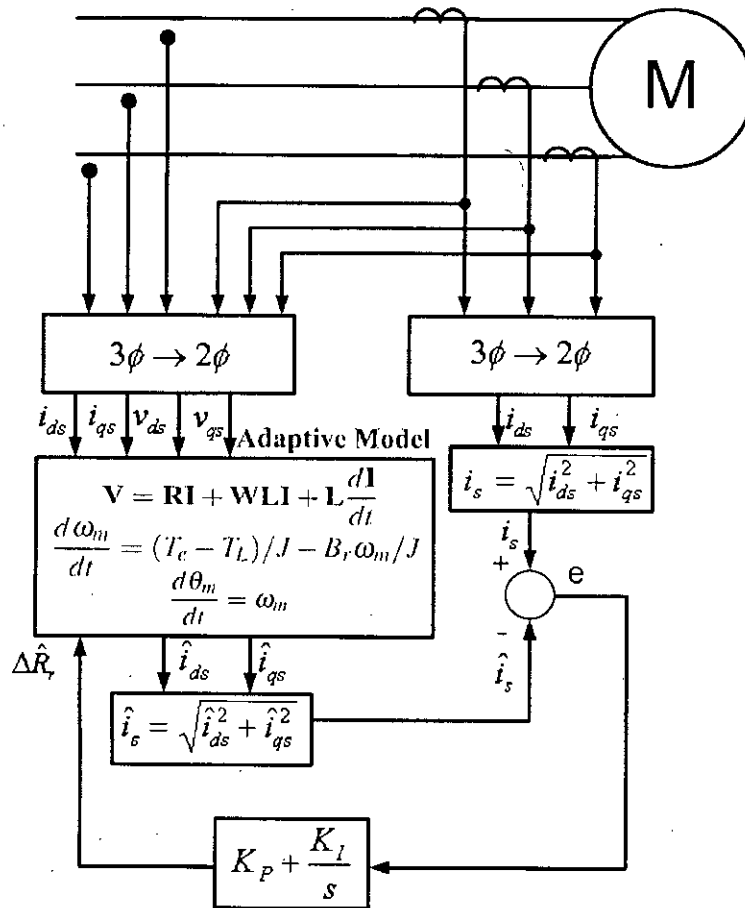


Figure 3.1: Rotor resistance estimation by the adaptive scheme

**Step2** : Calculate and save current magnitude from d-q currents.

**Step3** : Calculate the simulated current magnitude with the motor three phase input voltages available at that instance, test parameters and zero initial currents for a duration of 3 seconds.

**Step4** : Compare the last simulated current magnitude at the end of 3 second and captured current magnitude and save the error value.

**Step5** : Update the Rotor resistance in the simulation model according to the PI block and the error value.



**Step6** : If there is any update, then change the resistance or keep it on its previous value.

**Step7** : Go to step 1.

The detailed explanation of the steps are explained hereafter.

### **3.2.1 Sampling Step**

The three phase voltages and currents are sampled to the computer and a detailed adaptive model for the motor is established, where the nameplate parameters and the no load and blocked rotor test data are used. For the simulation the same model (3.1)-(3.5) is used to get the real stator current magnitude for a constant load.

### **3.2.2 The Change of Resistance Step**

The stator currents for changing the rotor resistance to different percentage of increment and decrement are calculated by the motor model and stored to estimate the change of rotor resistance by the adaptation model later. These currents act as if the current is found from the actual motor. For hardware in loop scheme the current from the physical motor is found through data acquisition card. These currents are used to calculate the actual current magnitude. This current magnitude is then compared with that of adaptive model.

### **3.2.3 Runge-Kutta Solution Step**

The state model is solved numerically with runge-kutta method for a short period of time. The simulation starts from transient state with zero initial values for the variables. From the simulation the direct axis and quadrature axis stator current, flux, torque and speed is found as a result.

### 3.2.4 Current Magnitude Calculation Step

When the model output goes to steady state then the simulated output current or the actual current from the motor found in the second step for changing rotor resistance of different percentage is applied to calculate the error in the adaptation process. Both the adaptive model and the real motor model gives the stator current in  $d - q$  reference frame from which the magnitude of the stator current is calculated as

$$i_s = \sqrt{i_{ds}^2 + i_{qs}^2} \quad (3.6)$$

The reference frame can be selected stator fixed, synchronously rotating or fixed at rotor. This output stator current from the adaptive model is compared with the real motor model and an error signal is generated.

### 3.2.5 Rotor Resistance Update Step

The three phase input voltages and the error are fed recurrently to the adaptive model to re-establish the motor parameters for the model.

$$\Delta \hat{R}_r = K_p(i_s - \hat{i}_s) + K_I \int (i_s - \hat{i}_s) dt \quad (3.7)$$

For re-establishing the model the error sign and magnitude plays a role and the rotor resistance is changed in a manner so that the error tends to a predefined threshold value.

### 3.2.6 Towards The Estimation Step

When the adaptive model gives almost the same output of the original motor the adaptation process ends. The threshold value for the error is not fixed. For fast adaptation it can be changed to an optimal value which depends on the motor size and application. The PI block parameters are also selected according to the requirement. According to the required accuracy the parameters vary to a certain limit. If the accuracy is very concerned then the

time for adaptation increases and the error threshold value and PI parameters are chosen accordingly. Though in practical situation the change of rotor resistance will happen slowly we change the original value abruptly with a greater percentage and observe the response time and accuracy of the algorithm.

Thus the whole adaptive scheme works. The simulation is done for several different rated motors. The constants used in the model is fixed through trial and error method, so that the optimum constants work for any motor in the simulation.

# Chapter 4

## Simulation Results

The simulation results for the model is presented. Simulation for different size of motors in respect of power capability is shown. Simulation for different reference models are also presented. The simulated output of different variables with changing different parameters is presented. Changing the rotor resistance the magnitude of the  $d - q$  current vector is also shown. The percentage of error and the time to reach the changed value is analyzed. Different motors are used to validate the simulation output.

### 4.1 Simulating the Model for 1hp Motor from Experimental Test Data

A 1hp three phase induction motor was selected for extracting the test data. These test results were used in the simulation and the results from the simulation are analyzed. The test result for the 1hp motor is given in Table 4.1.

Table 4.1: The test data for an 1hp motor

Parameter	Value	Unit
$R_s$	13.1	$\Omega$
$R_r$	10.71	$\Omega$
$L_{sl}$	32.8	$mH$
$L_{rl}$	32.8	$mH$
$L_m$	570	$mH$
$J$	0.01	$Kgm^2$
$B_m$	0.01	—
$T_L$	2.5	$Nm$
$p$	4	—

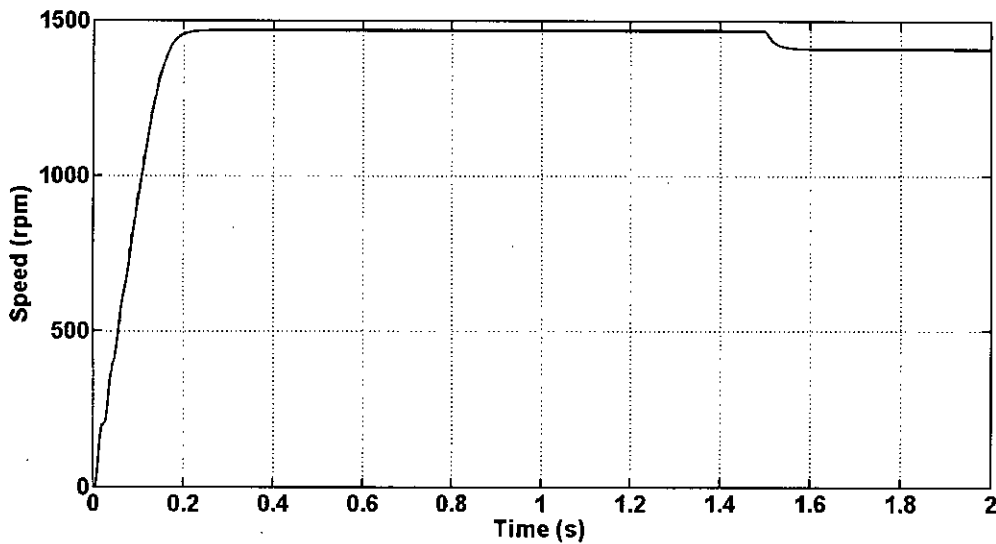


Figure 4.1: The speed of an 1hp motor with the full load applied on 1.5s

The simulation results for an 1 horse power motor is given in Figures 4.1 to 4.14.

The transient portion and the change in speed due to application of load is shown in Figure 4.1

The transient portion of the current is shown in Figure 4.2 The change of current magnitude due to change of load is shown in Figure 4.3

The  $d - q$  currents and the magnitude of the  $d - q$  current vector summation viewed in synchronous and rotor reference frame is shown in Figure 4.4 and 4.5

The transient portion and the change in torque due to application of load is shown in Figure 4.14

The transient portion of the current is shown in Figure 4.7

The change of current magnitude due to change of load is shown in Figure 4.8

The  $d - q$  fluxes viewed in synchronous and rotor reference frame is shown in Figure 4.9 and 4.10

The  $d - q$  voltages viewed in stator, synchronous and rotor reference frame is shown in Figure 4.11 , 4.12 and 4.13

The torque against speed is shown in Figure 4.14

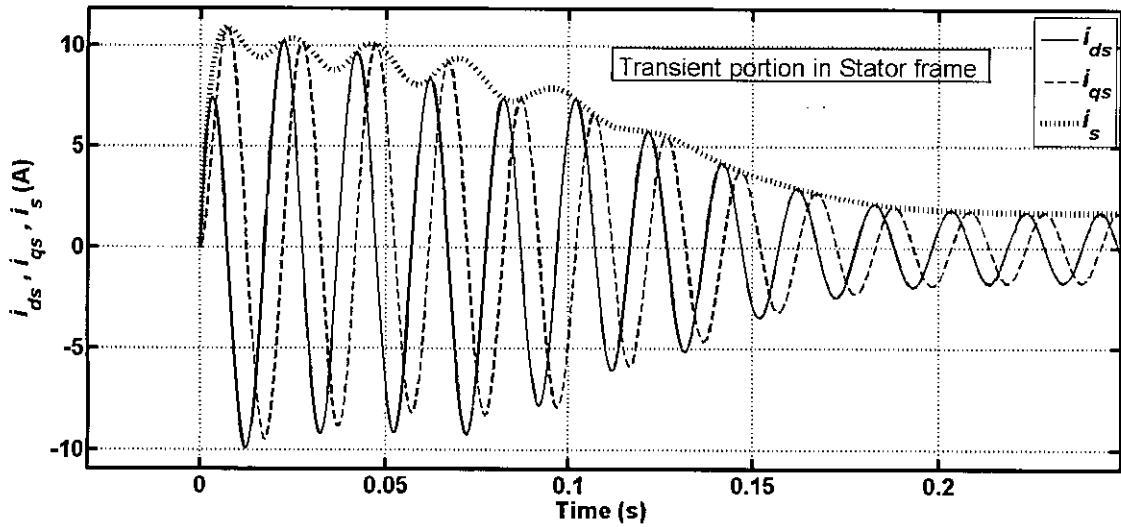


Figure 4.2: The transient portion of the  $d - q$  currents and the magnitude of the currents for an 1hp motor

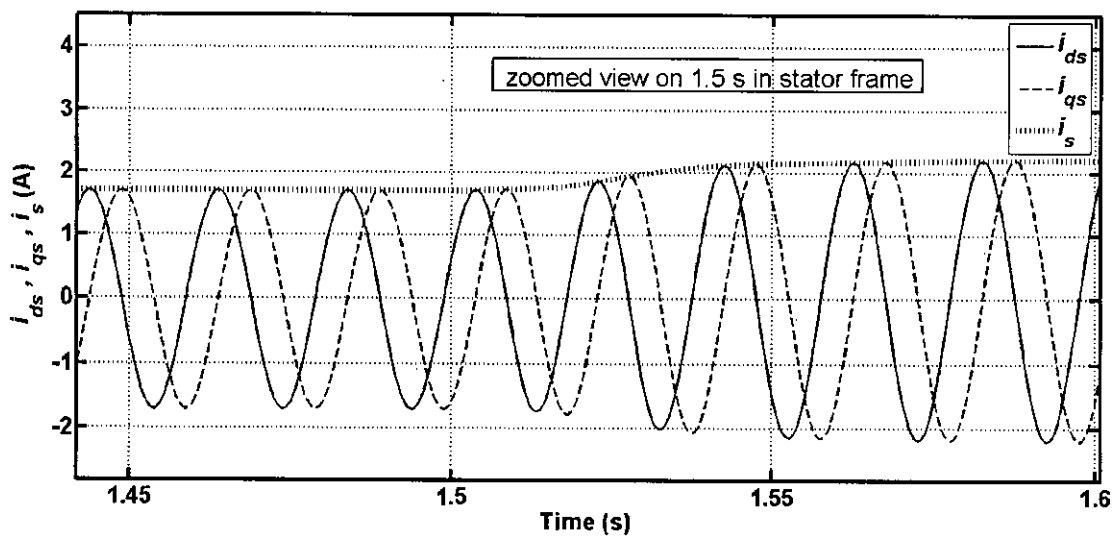


Figure 4.3: The change of current magnitude while the full load is applied for an 1hp motor

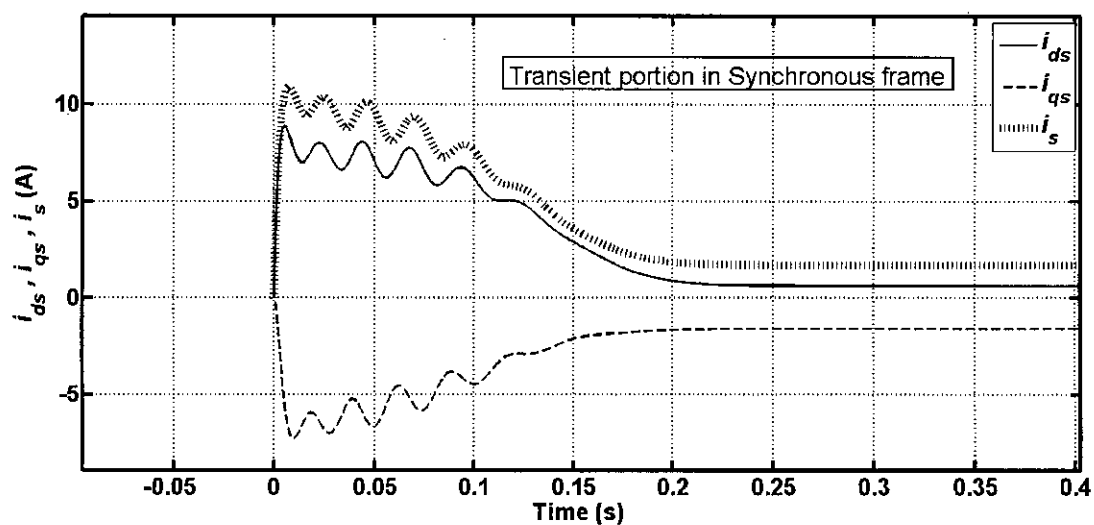


Figure 4.4: The  $d - q$  currents in synchronous reference frame while the full load is applied on 1.5 s for an 1hp motor

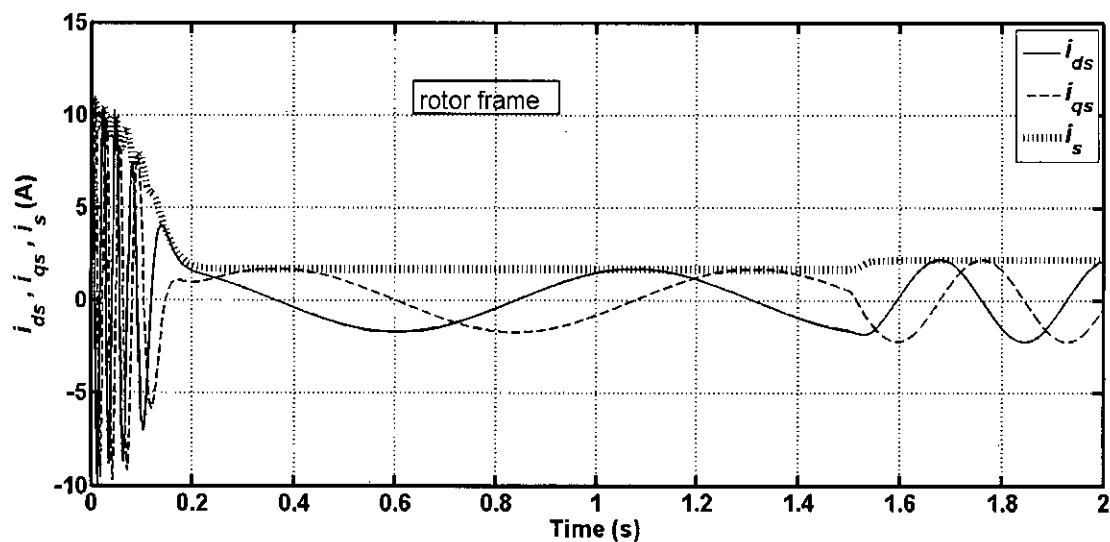


Figure 4.5: The  $d - q$  currents in rotor reference frame while the full load is applied on 1.5 s for an 1hp motor

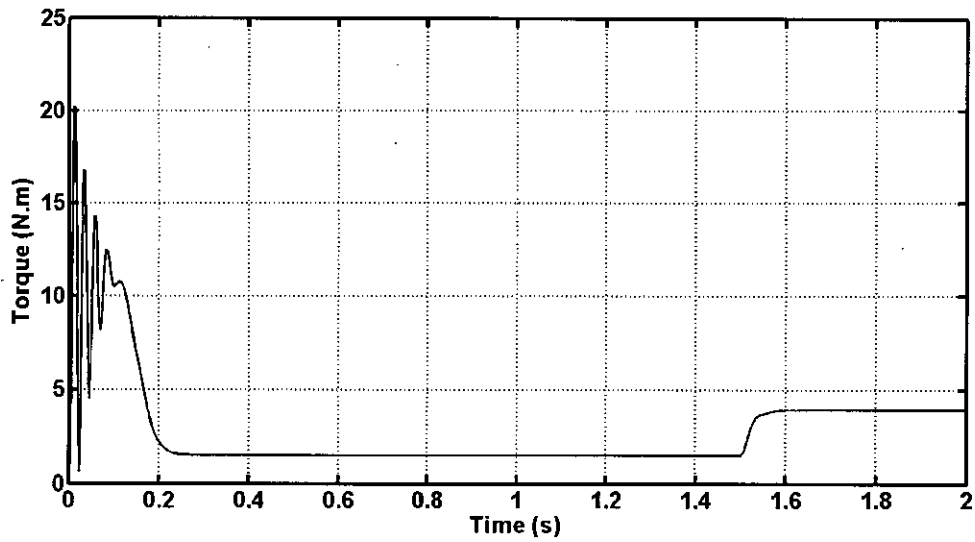


Figure 4.6: Transient and steady state portion of the torque while the full load is applied on 1.5s for an 1hp motor

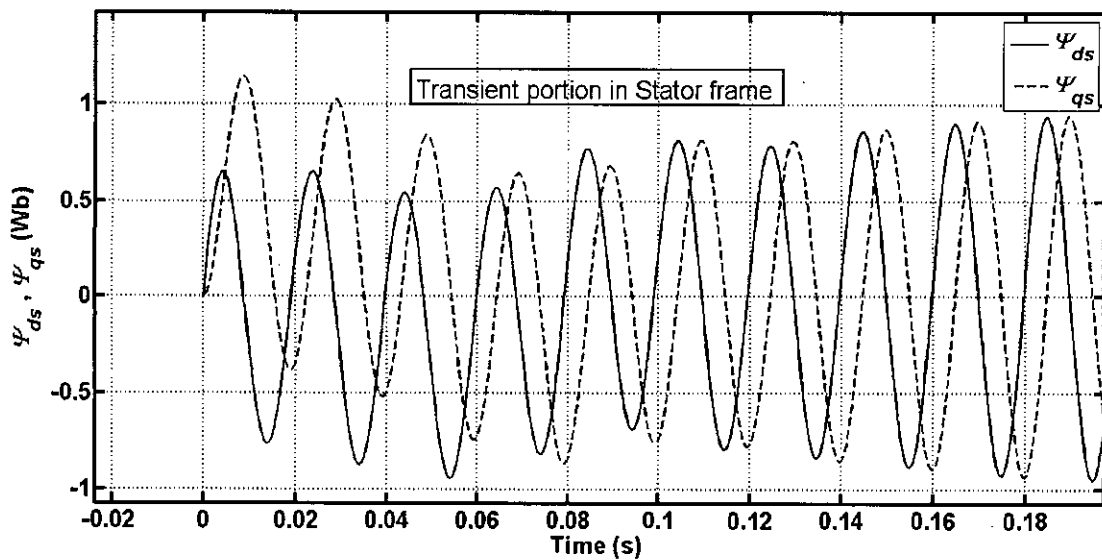


Figure 4.7: The transient portion of the  $d-q$  fluxes



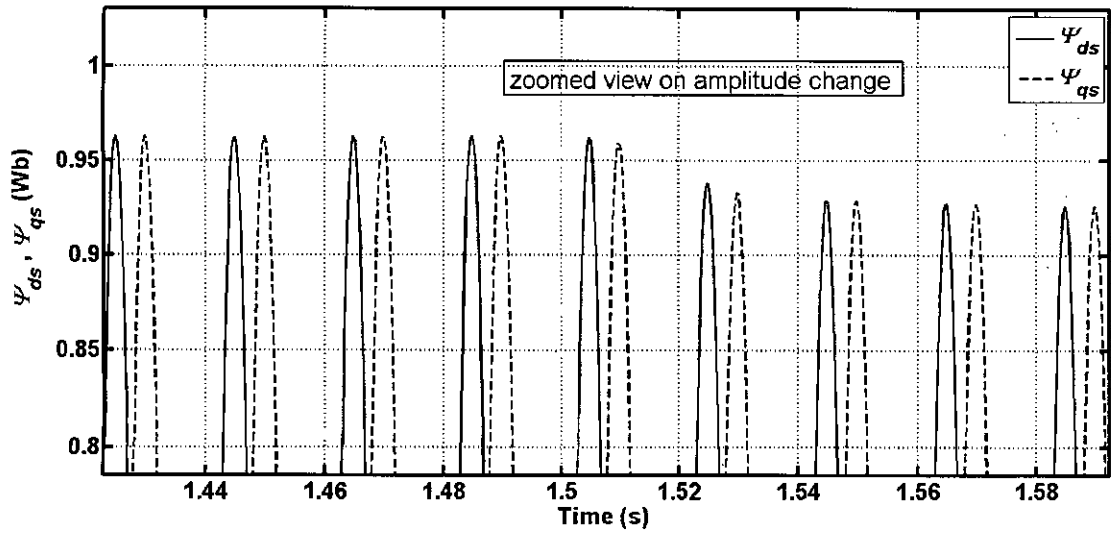


Figure 4.8: The change of flux magnitude while the full load is applied for an 1hp motor

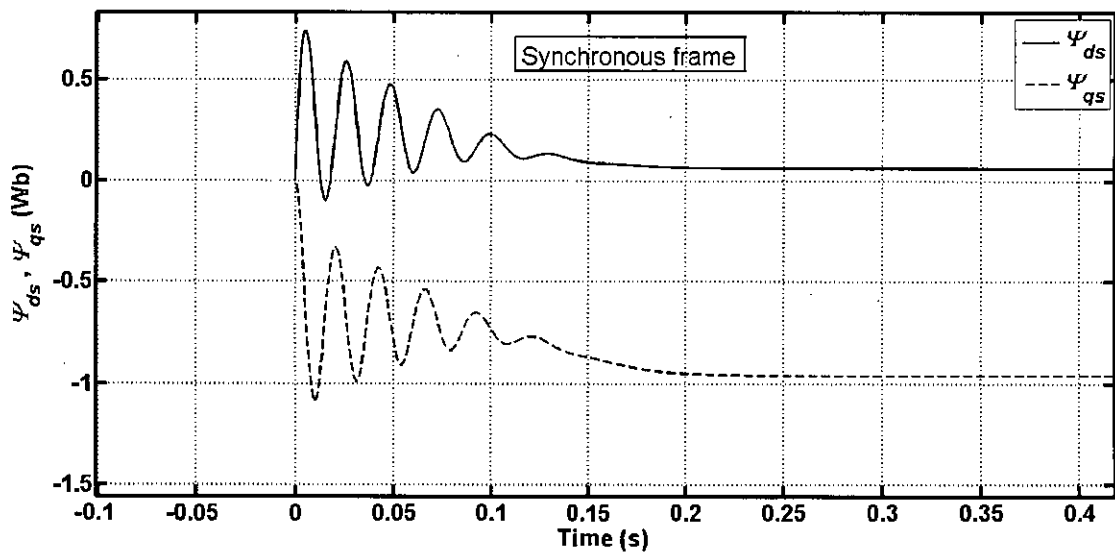


Figure 4.9: The  $d-q$  fluxes in synchronous frame while the full load is applied on 1.5 s for an 1hp motor

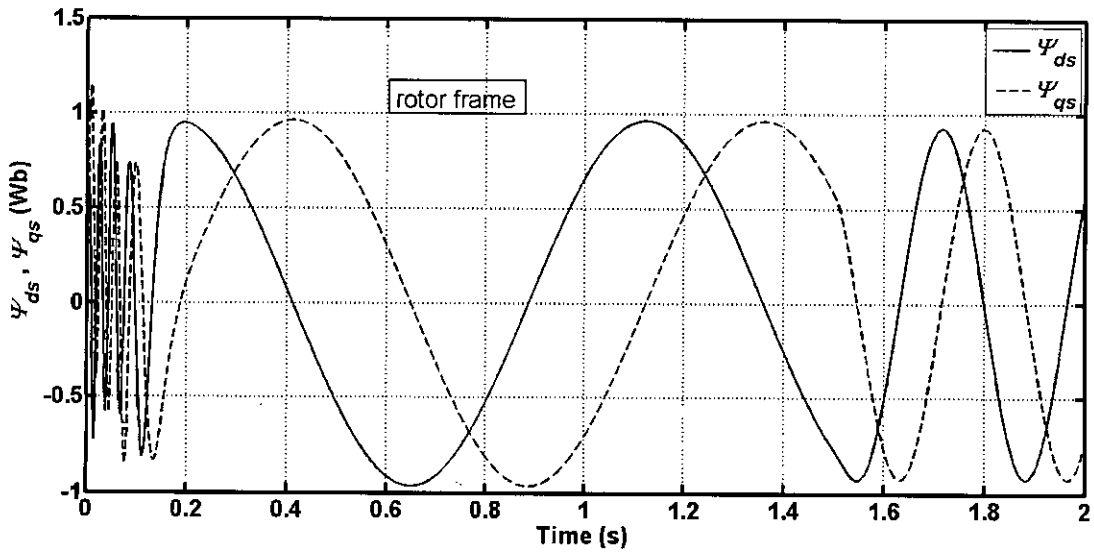


Figure 4.10: The  $d - q$  fluxes in rotor frame while the full load is applied on 1.5 s for an 1hp motor

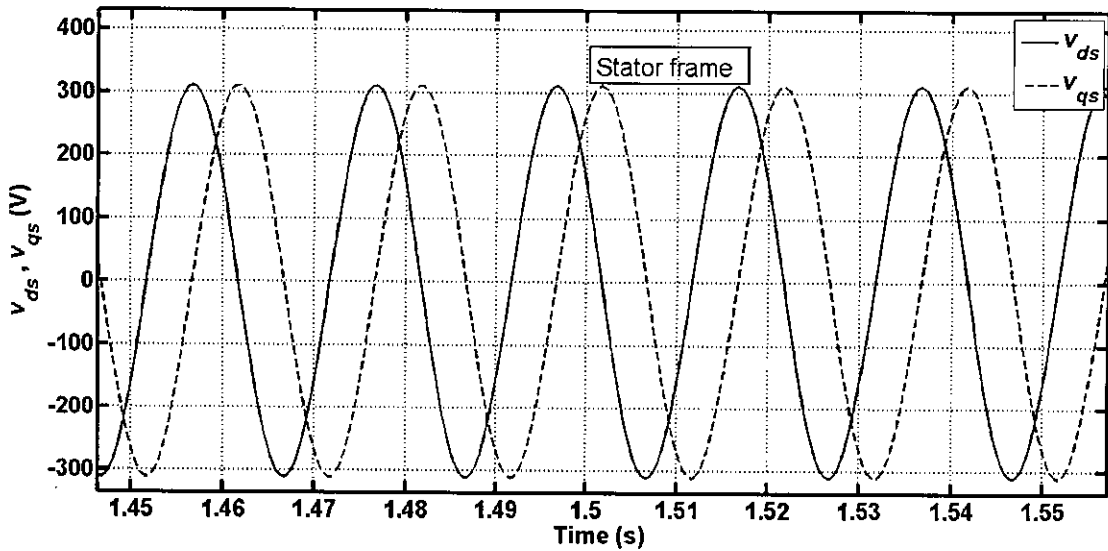


Figure 4.11: The  $d - q$  stator voltages in stator reference frame for an 1hp motor

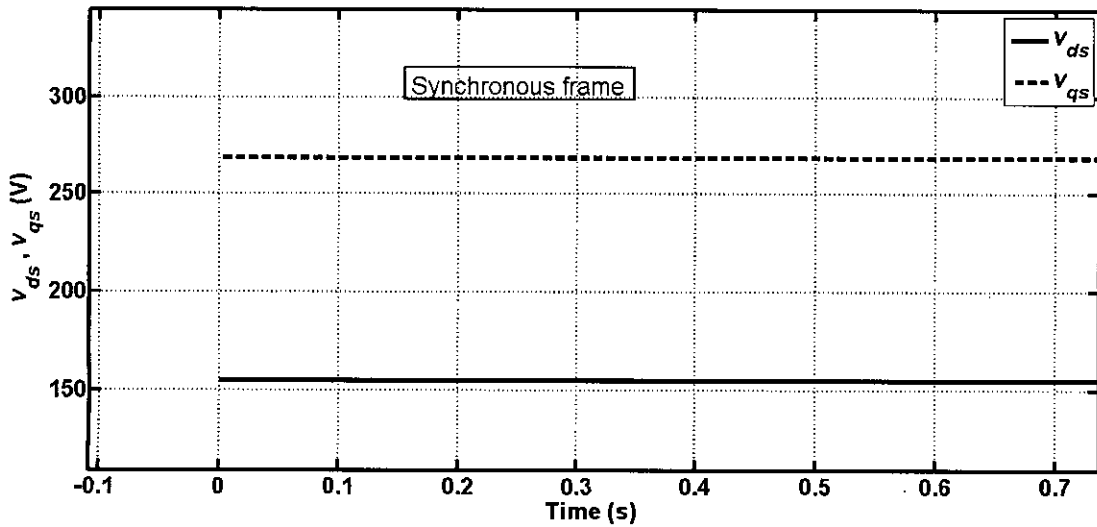


Figure 4.12: The  $d-q$  stator voltages in synchronous reference frame for an 1hp motor

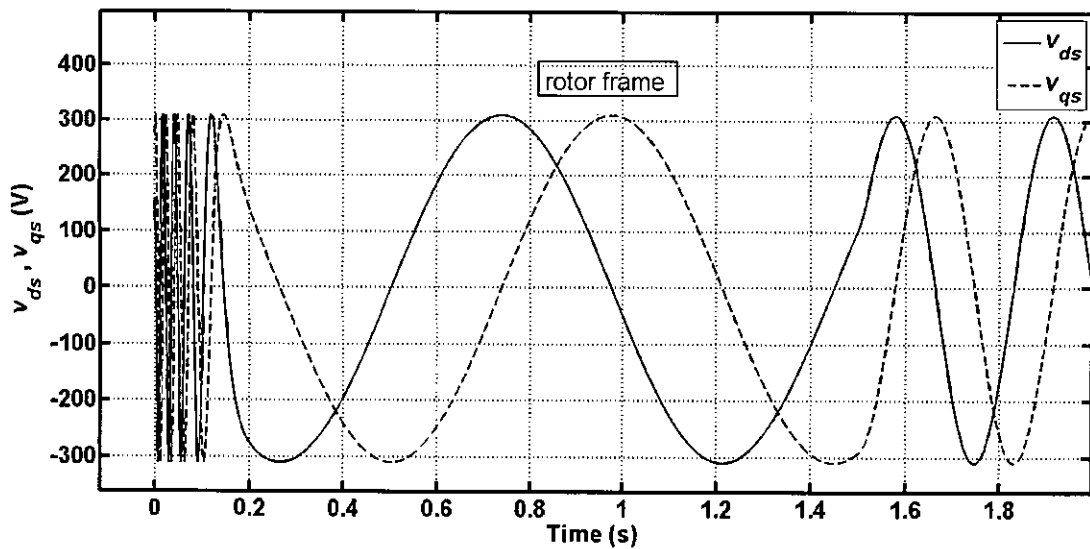


Figure 4.13: The  $d-q$  stator voltages in rotor reference frame for an 1hp motor

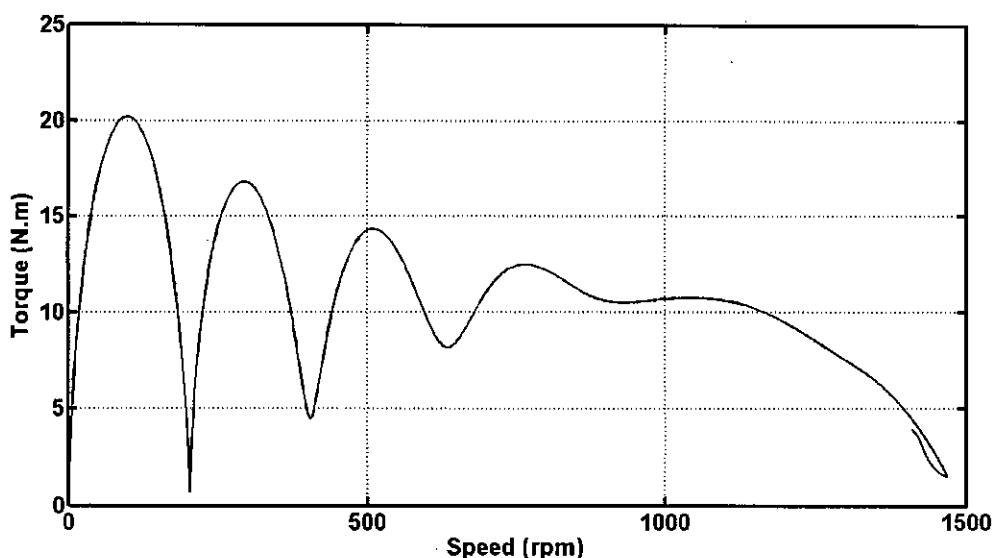


Figure 4.14: The torque is shown against speed for an 1hp motor

## 4.2 Simulating the Change of Rotor Resistance While Tracking the Change for the Test Data of an 1hp Motor

To observe whether the adaptive scheme can track the change of rotor resistance some simulations are done on different power rated motors. For simulation everything in the computer a fixed model for the motor is used. The three phase currents from the fixed model is converted to two phase currents and then the magnitude of the  $d - q$  current vector sum is calculated. This current magnitude is compared with the same output from the adaptive model. The error is fed back to the adaptive model to update the rotor resistance of the adaptive model. The fixed model output is supplied to the comparator with 2% of error.

The resistance of the fixed model is changed to 150% of it's initial value and the corresponding output current from the fixed model is fed to the comparator. The adaptive scheme is simulated with the change of rotor resistance. The resistance then changed back to its initial value, then again changed to 80% of it's initial value and then back to initial value again. The performance is shown in Figure 4.15 to 4.18.

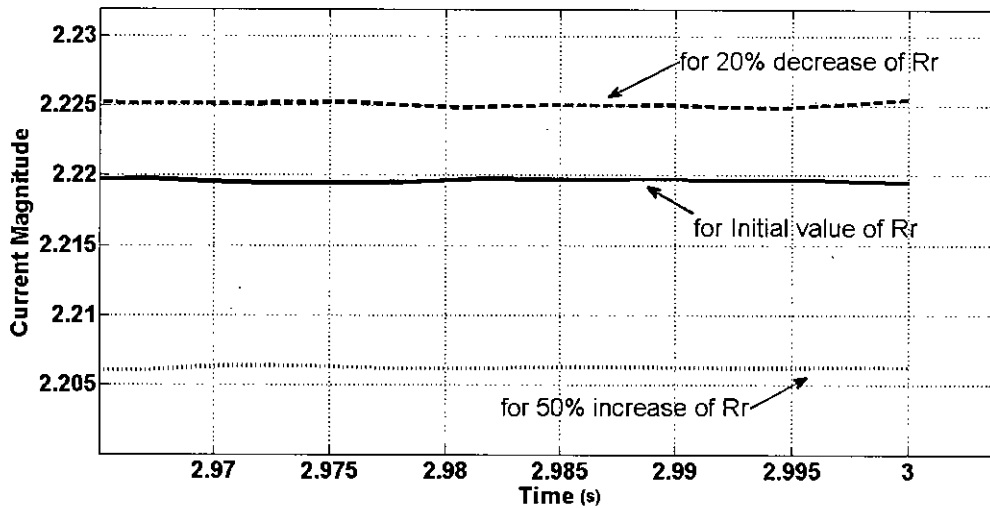


Figure 4.15: The change of current due to change of rotor resistance for an 1hp motor

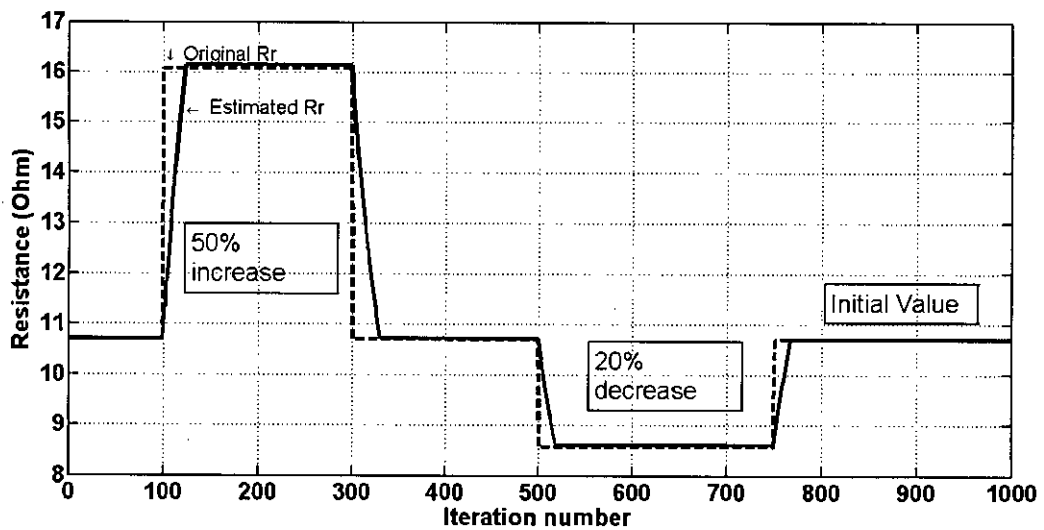


Figure 4.16: The estimated rotor resistance is tracking the change made in the simulation for an 1hp motor

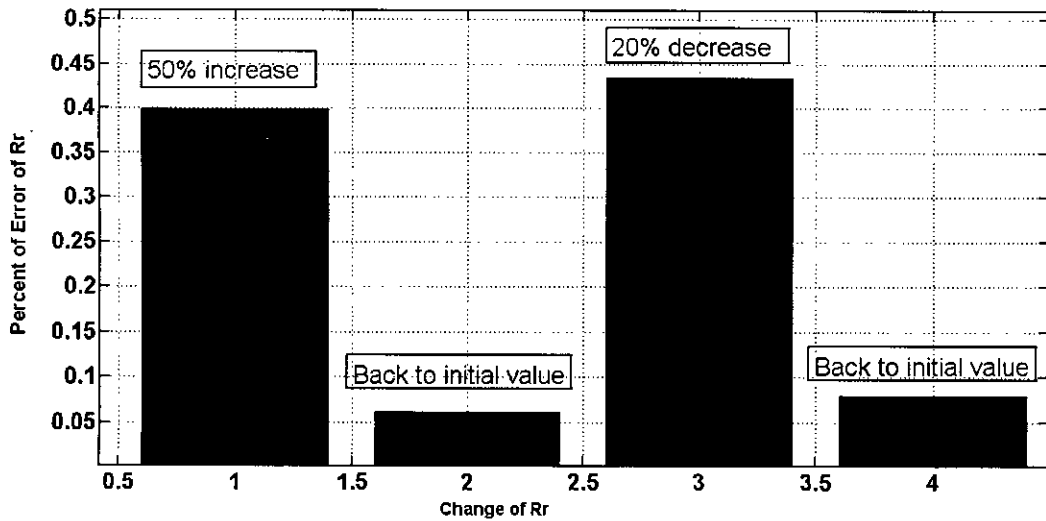


Figure 4.17: The percentage of error while tracking the change made in the simulation for an 1hp motor

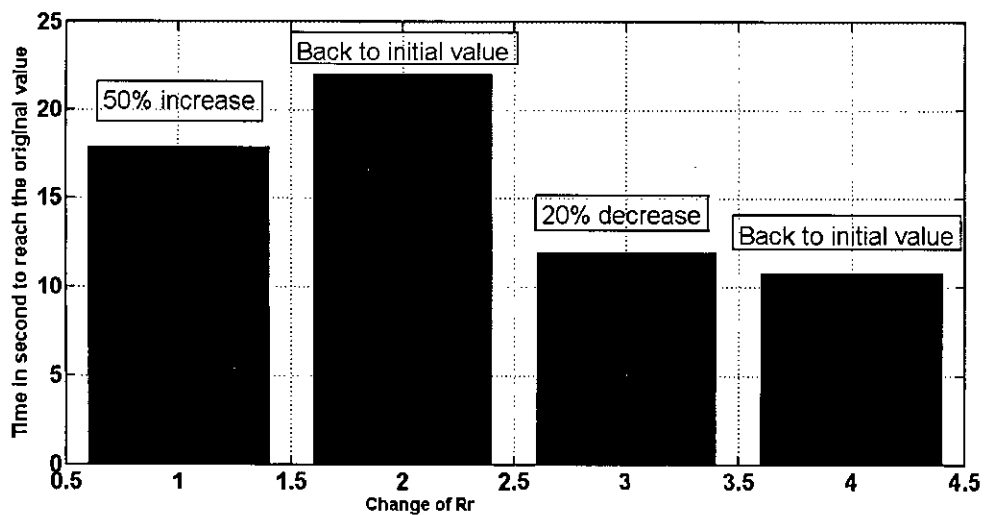


Figure 4.18: The time to reach the original changed value while tracking the change made in the simulation for an 1hp motor

Table 4.2: The test data for a 3hp motor

Parameter	Value	Unit
$R_s$	3.5	$\Omega$
$R_r$	3.16	$\Omega$
$L_{sl}$	6.6	$mH$
$L_{rl}$	6.8	$mH$
$L_m$	268	$mH$
$J$	0.2	$Kgm^2$
$B_m$	0.02	—
$T_L$	7	$Nm$
$p$	4	—

### 4.3 Simulating the Model for 3hp Motor

A 3hp three phase induction motor is also used for simulation. The test results [20] were used in the simulation and the results from the simulation are analyzed. The test result for the 3hp motor is given in Table 4.2.

The simulation results for a 3 horse power motor is given in Figures 4.19 to 4.31.

### 4.4 Simulating the Change of Rotor Resistance While Tracking the Change for the Test Data of a 3hp Motor

To observe whether the adaptive scheme can track the change of rotor resistance simulations for a 3hp motor are also done. As for the 1hp motor a fixed model for the 3hp motor is used. The three phase currents from the fixed model is converted to two phase currents and then the magnitude of the  $d - q$  current vector sum is calculated. This current magnitude is compared with the same output from the adaptive model. The error is fed back to the adaptive model to update the rotor resistance of the adaptive model. The fixed model output is supplied to the comparator with 2% of error.

As in the 1hp motor simulation the resistance of the fixed model is changed to 150% of it's initial value and the corresponding output current from the fixed model is fed to the comparator. The adaptive scheme is simulated with the change of rotor resistance. The resistance then changed back to its initial value, then again changed to 80% of it's initial

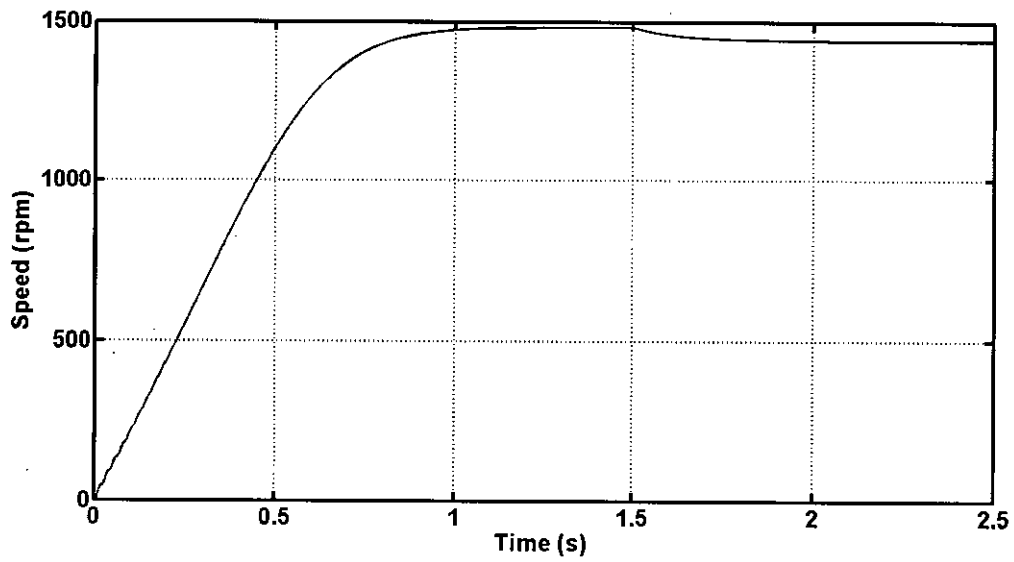


Figure 4.19: The speed of a 3hp motor with the full load applied on 1.5s

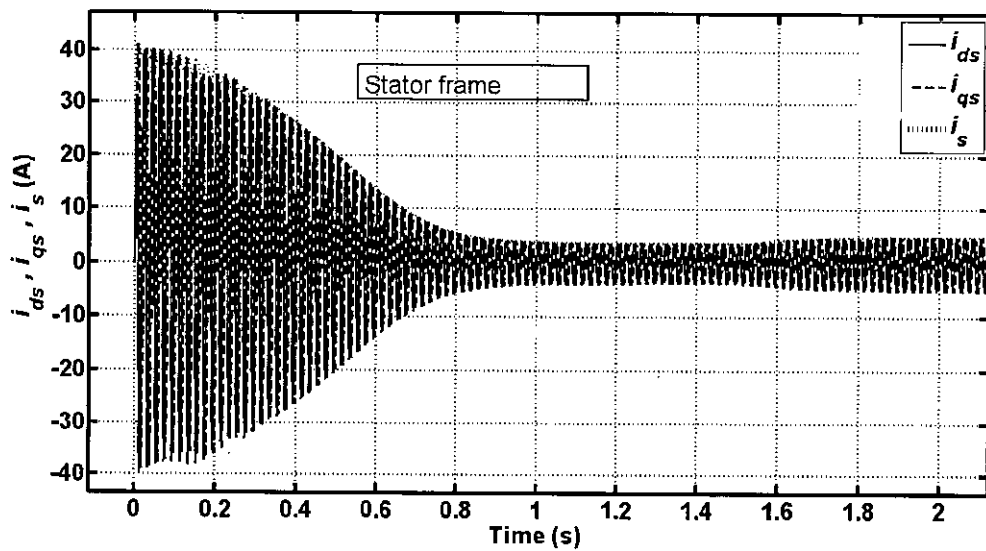


Figure 4.20: The change of current magnitude while the full load is applied for a 3hp motor



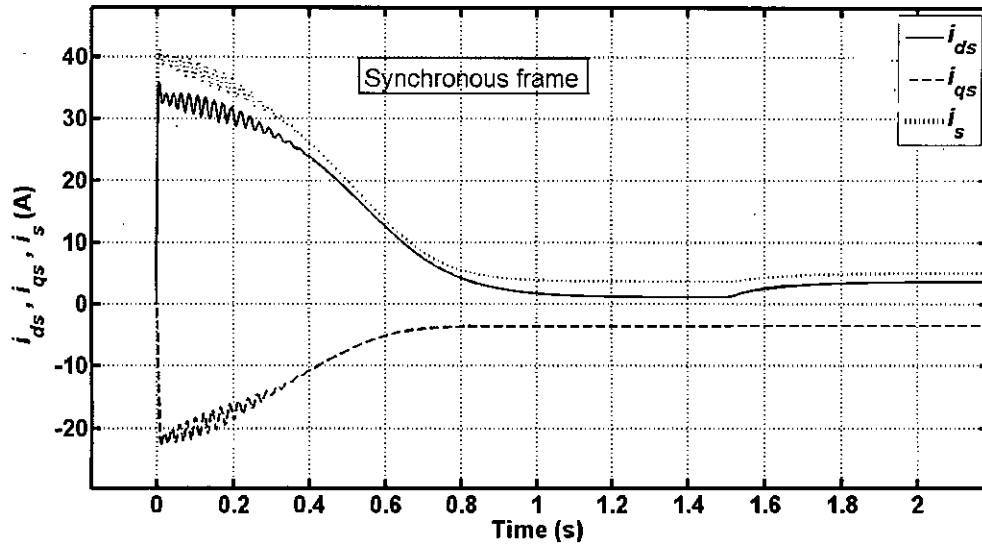


Figure 4.21: The  $d - q$  currents in synchronous reference frame while the full load is applied on 1.5 s for a 3hp motor

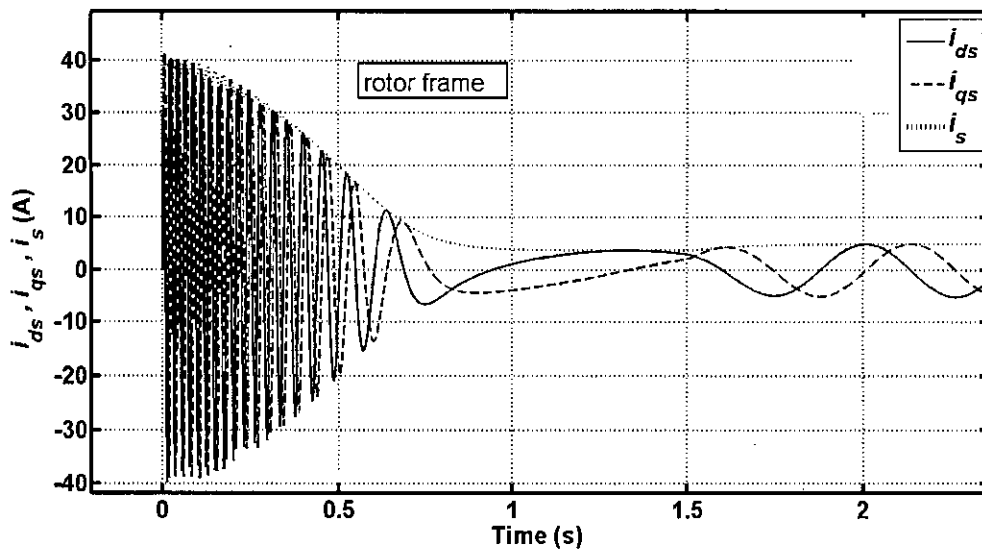


Figure 4.22: The  $d - q$  currents in rotor reference frame while the full load is applied on 1.5 s for a 3hp motor

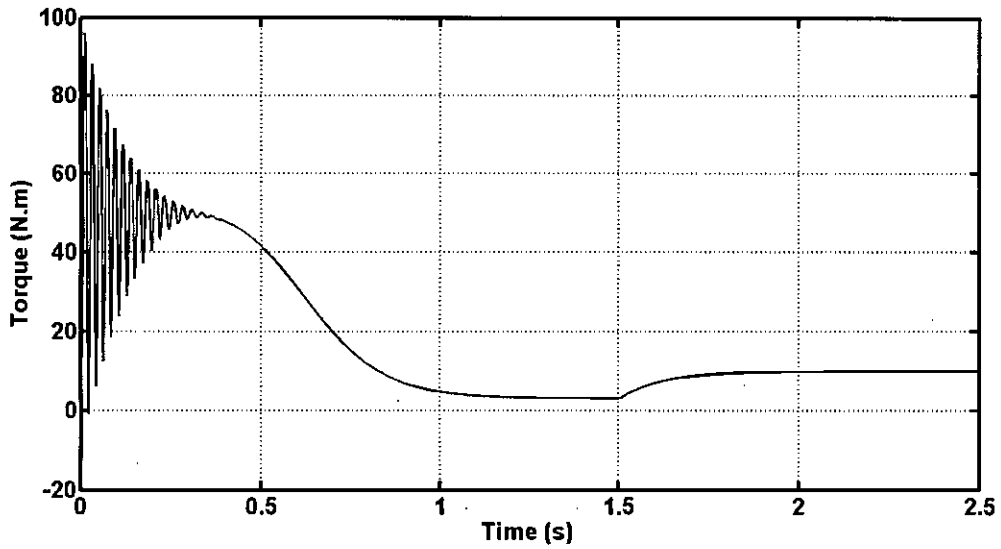


Figure 4.23: Transient and steady state portion of the torque while the full load is applied on 1.5s for a 3hp motor

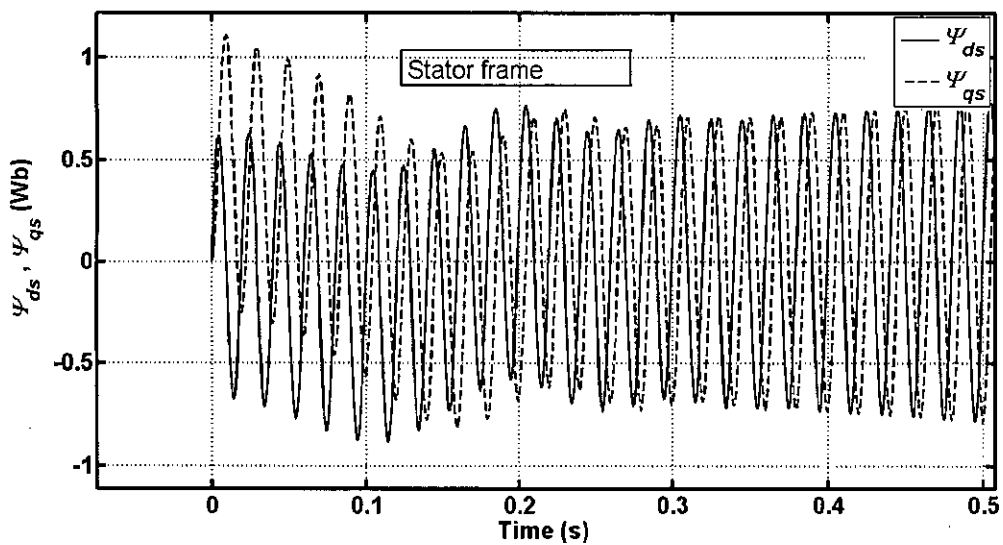


Figure 4.24: The transient portion of the  $d - q$  fluxes

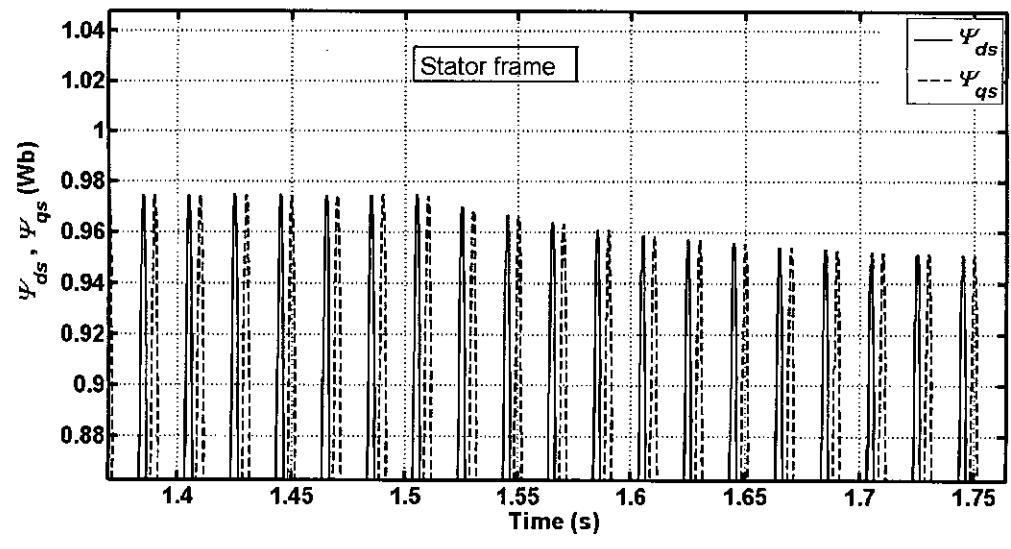


Figure 4.25: The change of flux magnitude while the full load is applied for a 3hp motor

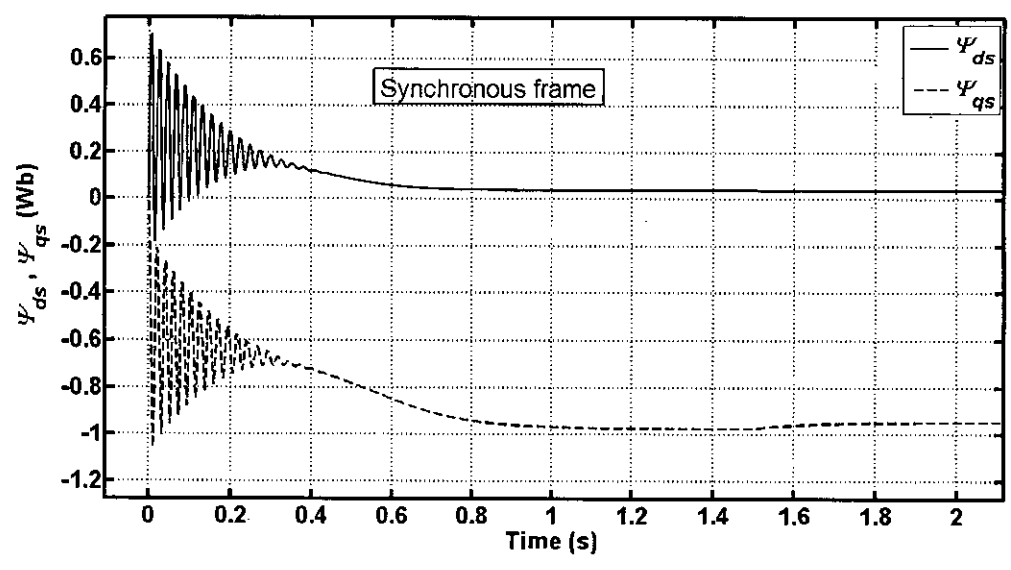


Figure 4.26: The  $d - q$  fluxes in synchronous frame while the full load is applied on 1.5 s for a 3hp motor

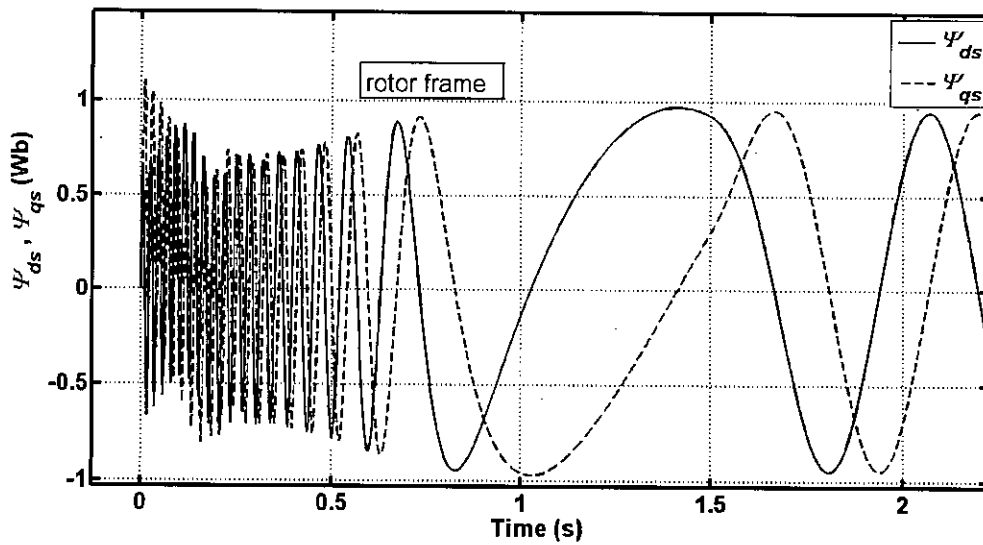


Figure 4.27: The  $d - q$  fluxes in rotor frame while the full load is applied on 1.5 s for a 3hp motor

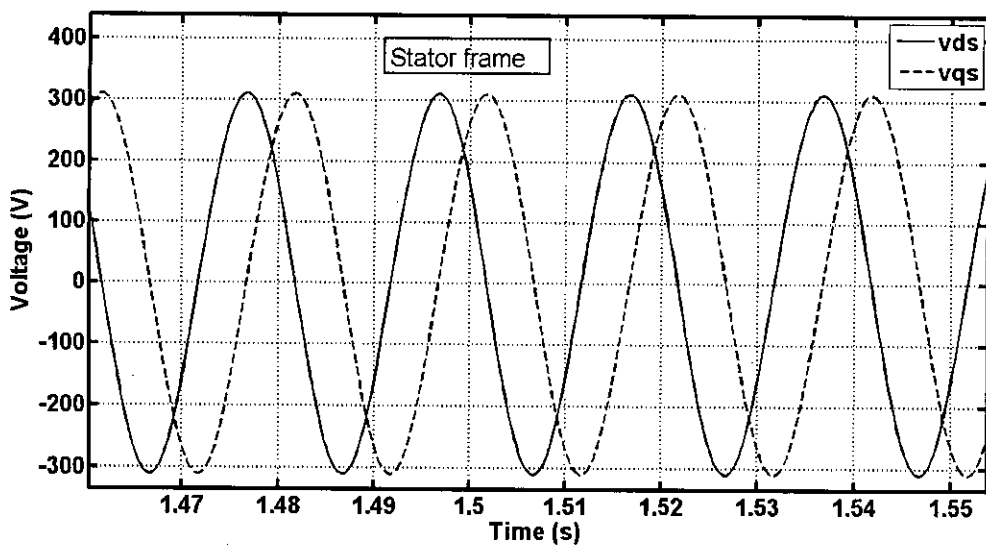


Figure 4.28: The  $d - q$  stator voltages in stator reference frame for a 3hp motor

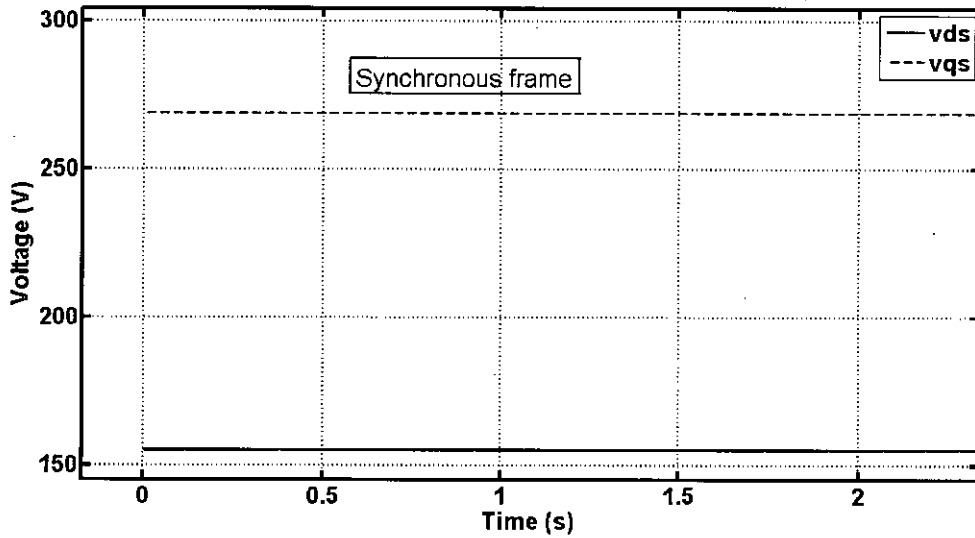


Figure 4.29: The  $d-q$  stator voltages in synchronous reference frame for a 3hp motor

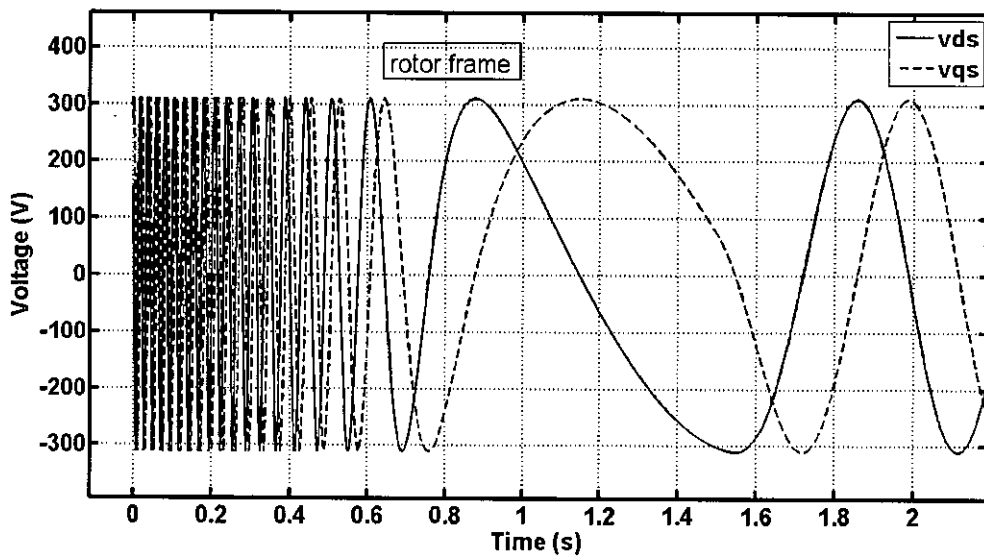


Figure 4.30: The  $d-q$  stator voltages in rotor reference frame for a 3hp motor

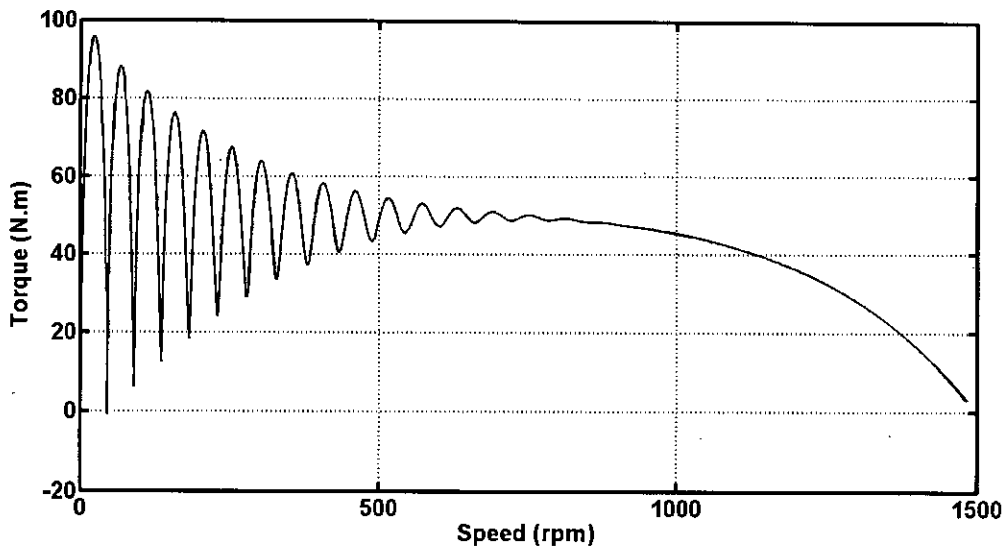


Figure 4.31: The torque is shown against speed for a 3hp motor

value and then back to initial value again. The performance is shown in Figure 4.32 to 4.35.

## 4.5 Simulating the Model for 5hp Motor

A 5hp three phase induction motor is also used for simulation. The test results [20] were used in the simulation and the results from the simulation are analyzed. The test result for the 5hp motor is given in Table 4.3.

The simulation results for a 5 horse power motor is given in Figures 4.36 to 4.48.

Table 4.3: The test data for a 5hp motor

Parameter	Value	Unit
$R_s$	2.5	$\Omega$
$R_r$	1.57	$\Omega$
$L_{sl}$	10.2	mH
$L_{rl}$	7.5	mH
$L_m$	198	mH
$J$	0.1	$\text{Kgm}^2$
$B_m$	0.02	—
$T_L$	11	Nm
$p$	4	—

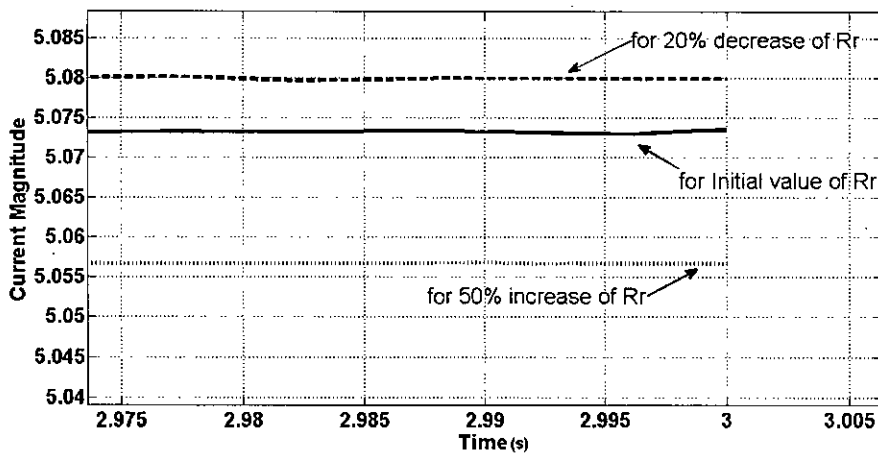


Figure 4.32: The change of current due to change of rotor resistance for a 3hp motor

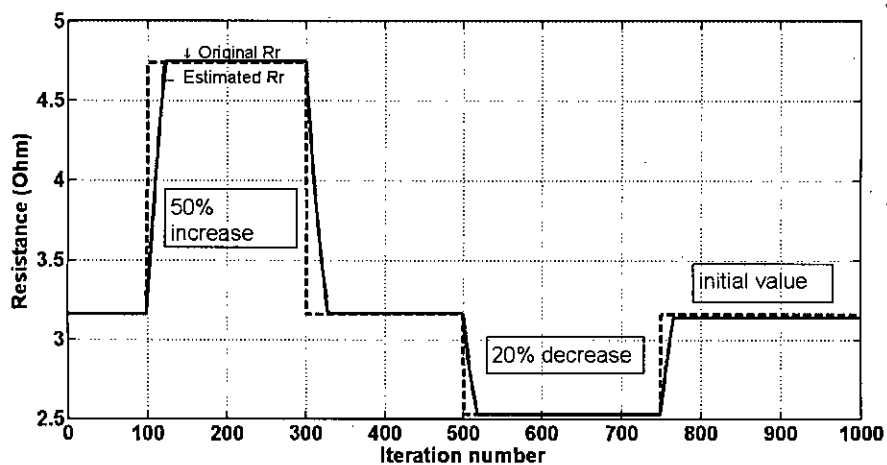


Figure 4.33: The estimated rotor resistance is tracking the change made in the simulation for a 3hp motor

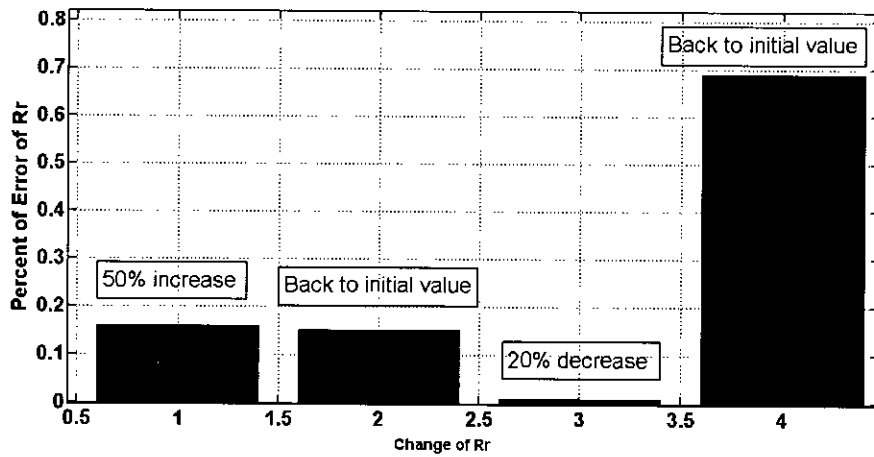


Figure 4.34: The percentage of error while tracking the change made in the simulation for a 3hp motor

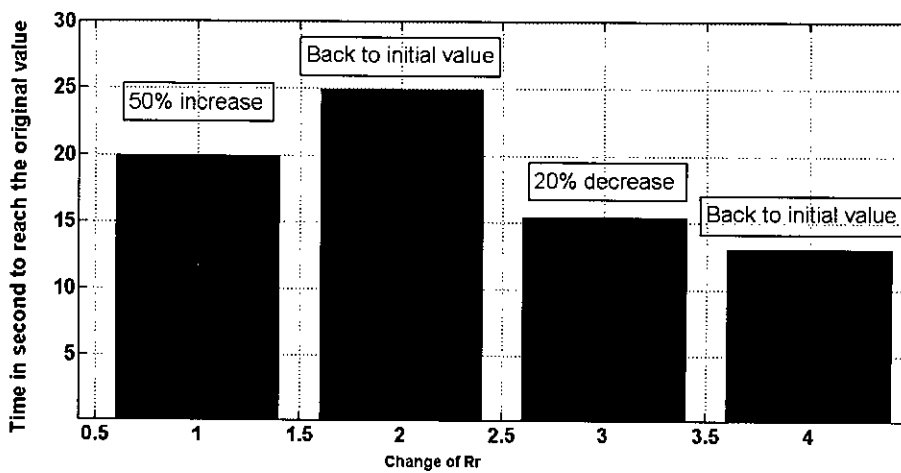


Figure 4.35: The time to reach the original changed value while tracking the change made in the simulation for a 3hp motor



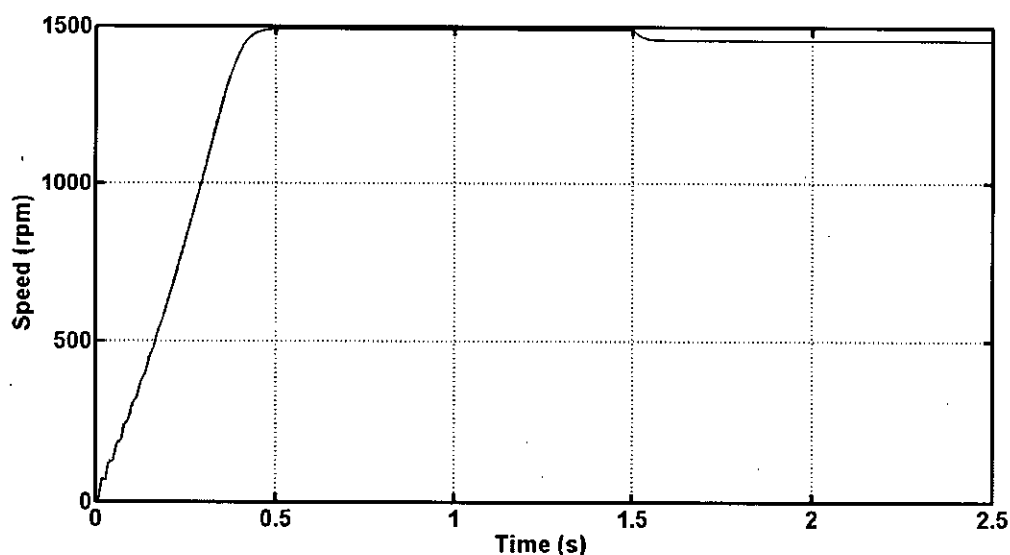


Figure 4.36: The speed of a 5hp motor with the full load applied on 1.5s

The transient portion of the speed is shown in Figure 4.36

## 4.6 Simulating the Change of Rotor Resistance While Tracking the Change for the Test Data of a 5hp Motor

To observe whether the adaptive scheme can track the change of rotor resistance simulations for a 5hp motor are also done. As for the 1hp motor a fixed model for the 5hp motor is used. The three phase currents from the fixed model is converted to two phase currents and then the magnitude of the  $d - q$  current vector sum is calculated. This current magnitude is compared with the same output from the adaptive model. The error is fed back to the adaptive model to update the rotor resistance of the adaptive model. The fixed model output is supplied to the comparator with 2% of error.

As in the 1hp motor simulation the resistance of the fixed model is changed to 150% of its initial value and the corresponding output current from the fixed model is fed to the comparator. The adaptive scheme is simulated with the change of rotor resistance. The resistance then changed back to its initial value, then again changed to 80% of its initial value and then back to initial value again. The performance is shown in Figure 4.49 to 4.52.

The same simulation is done for 1hp, 3hp and 5hp motors. The 1hp motor was bought

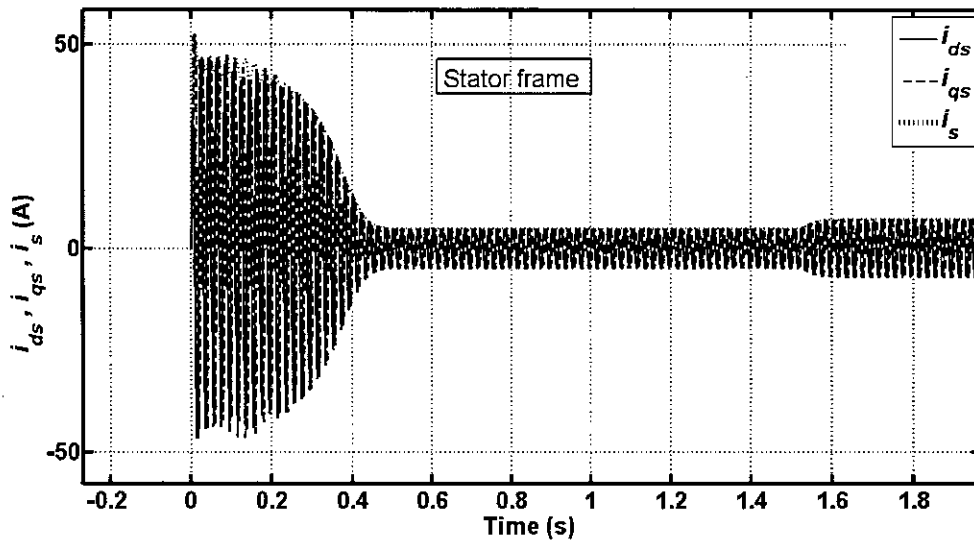


Figure 4.37: The change of current magnitude while the full load is applied for a 5hp motor

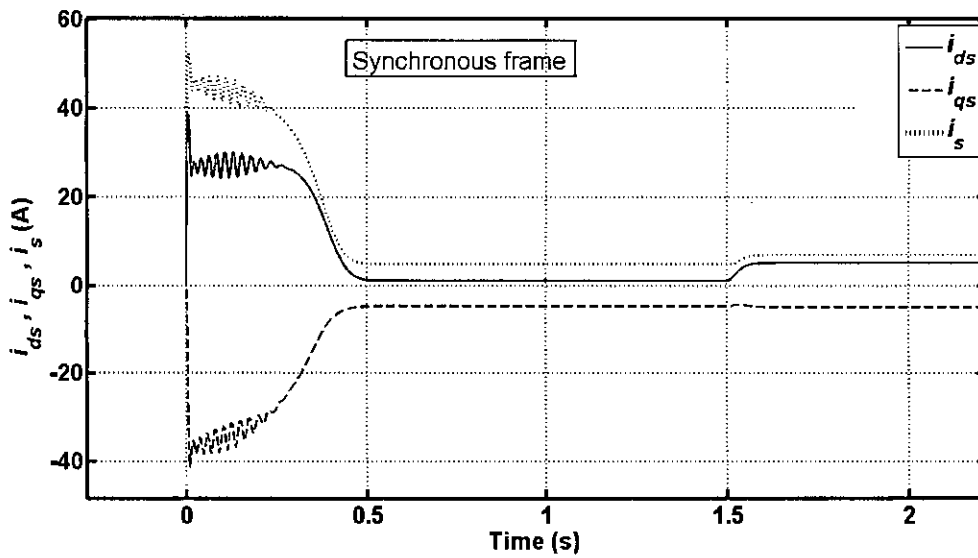


Figure 4.38: The  $d - q$  currents in synchronous reference frame while the full load is applied on 1.5 s for a 5hp motor

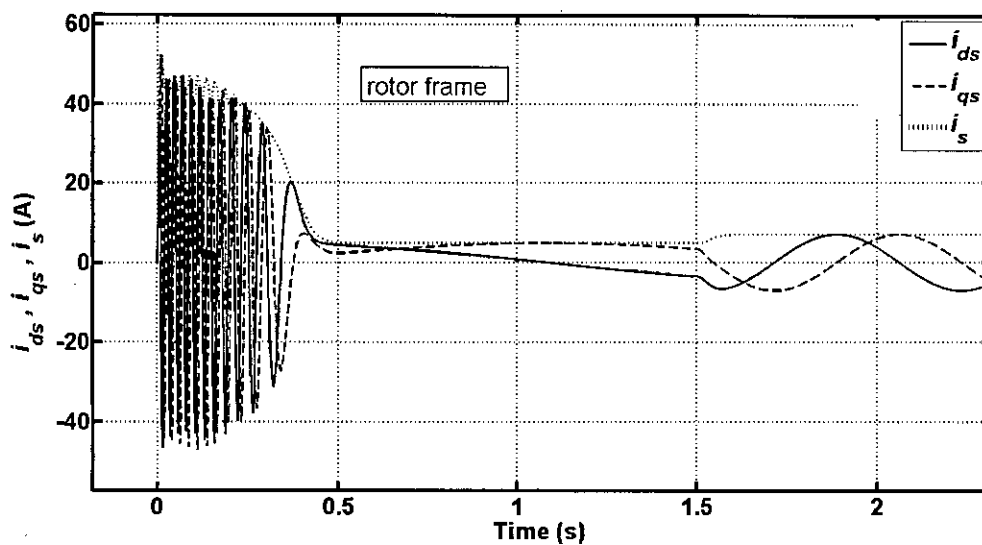


Figure 4.39: The  $d - q$  currents in rotor reference frame while the full load is applied on 1.5 s for a 5hp motor

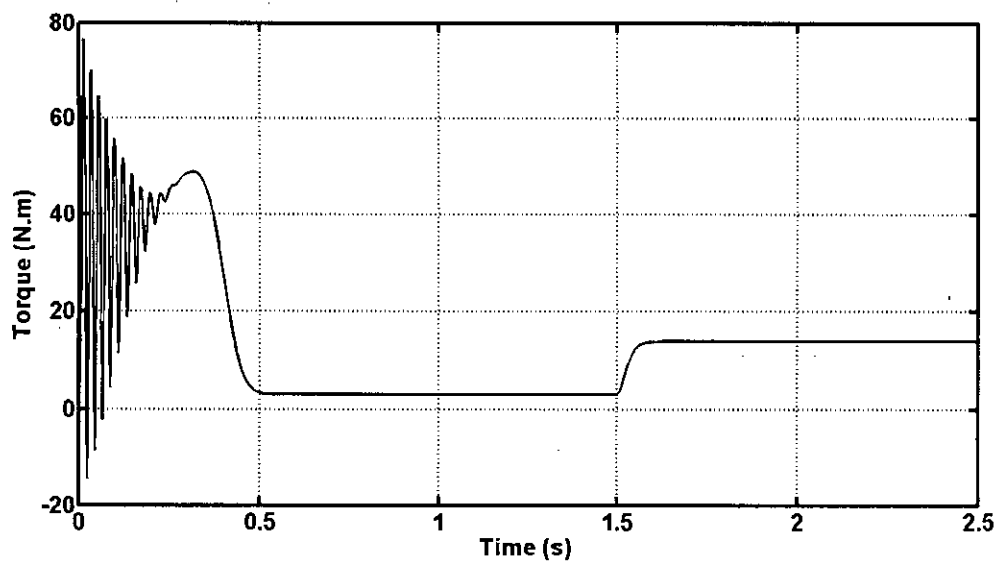


Figure 4.40: Transient and steady state portion of the while the full load is applied on 1.5s for a 5hp motor

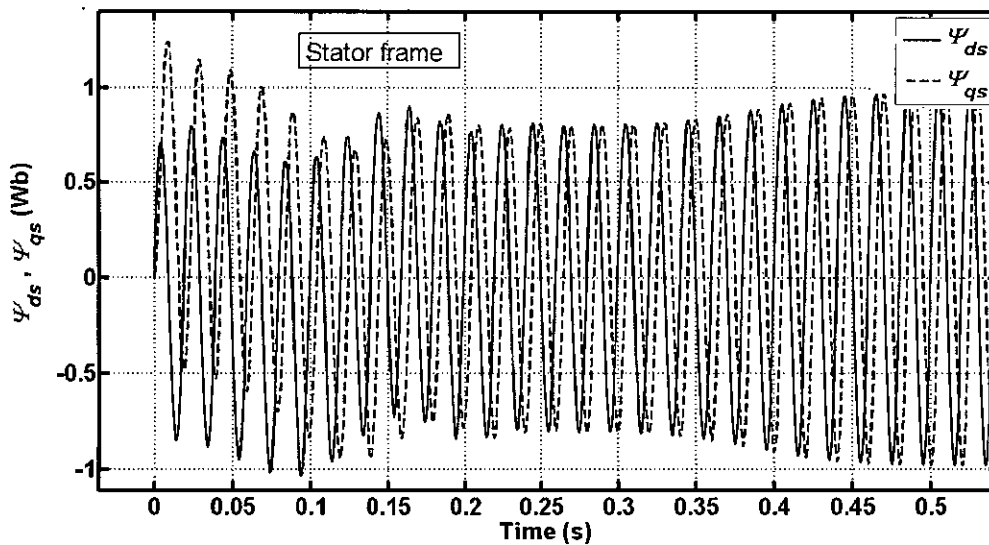


Figure 4.41: The transient portion of the  $d-q$  fluxes

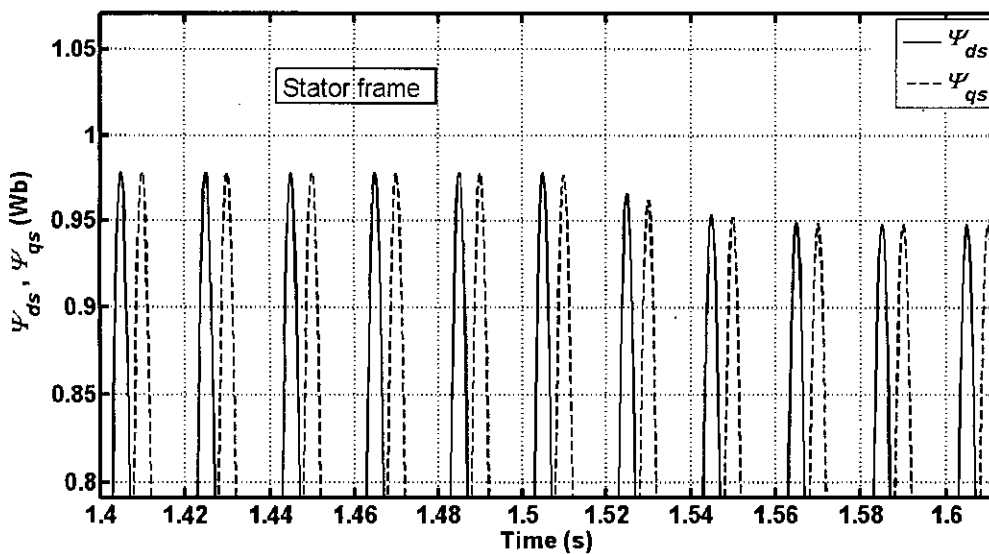


Figure 4.42: The change of flux magnitude while the full load is applied for a 5hp motor

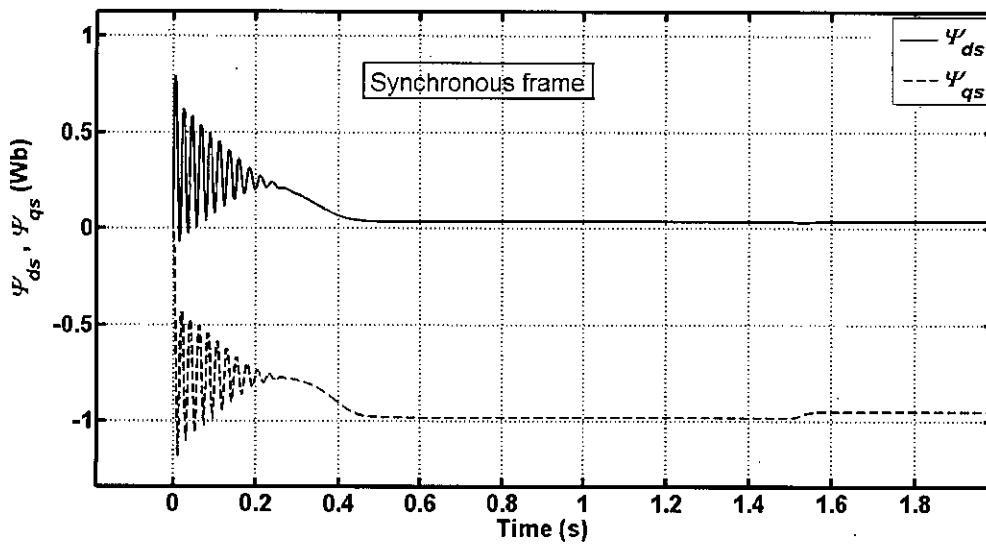


Figure 4.43: The  $d-q$  fluxes in synchronous frame while the full load is applied on 1.5 s for a 5hp motor

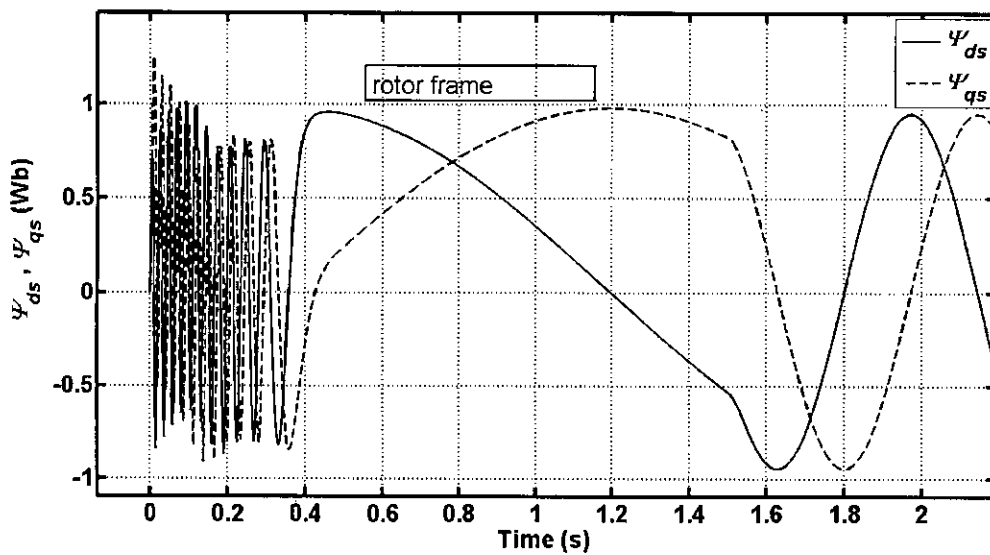


Figure 4.44: The  $d-q$  fluxes in rotor frame while the full load is applied on 1.5 s for a 5hp motor

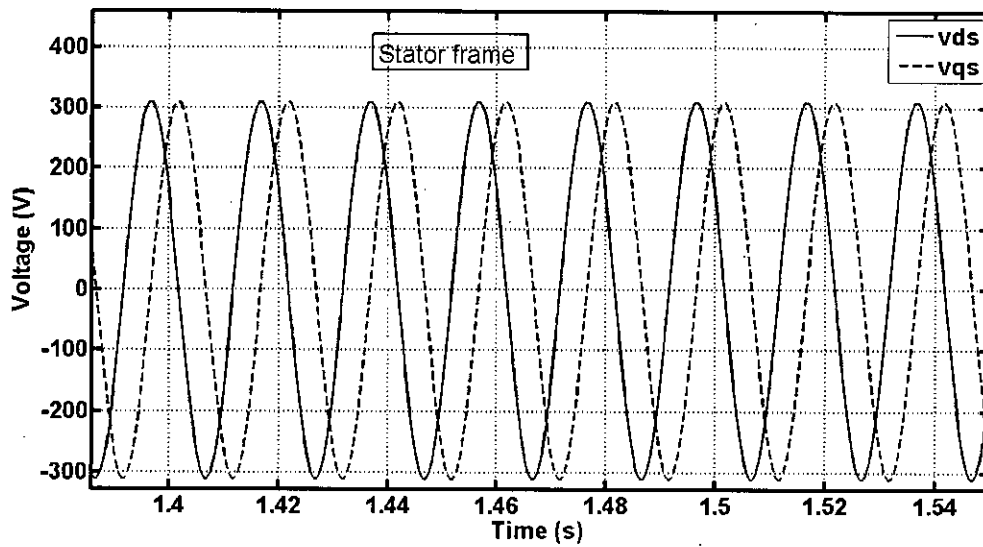


Figure 4.45: The  $d - q$  stator voltages in stator reference frame for a 5hp motor

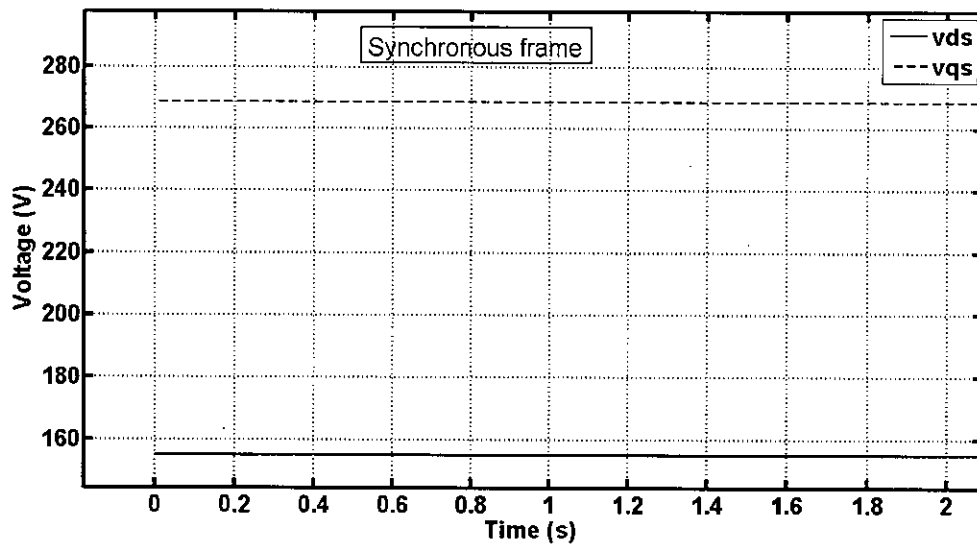


Figure 4.46: The  $d - q$  stator voltages in synchronous reference frame for a 5hp motor

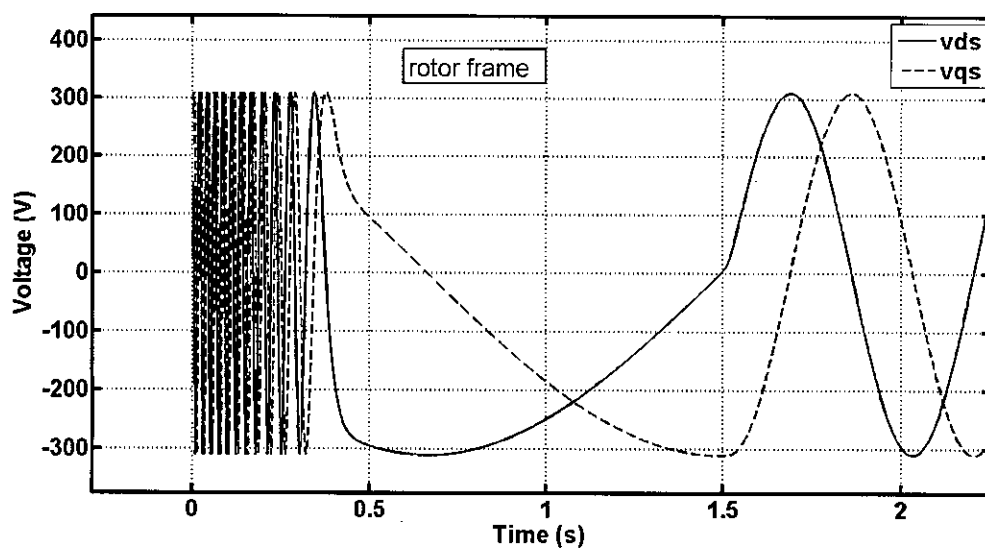


Figure 4.47: The  $d - q$  stator voltages in rotor reference frame for a 5hp motor

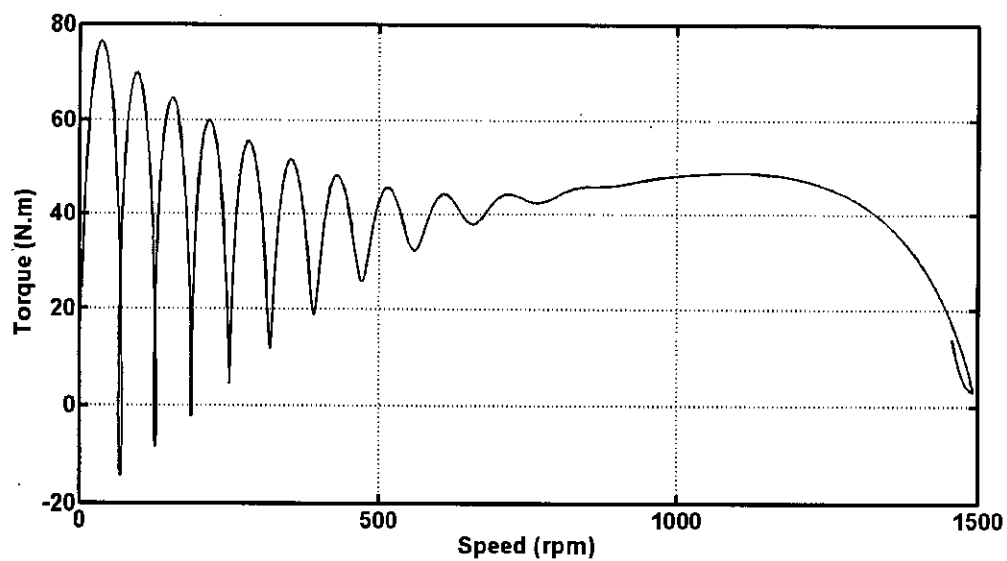


Figure 4.48: The torque is shown against speed for a 5hp motor

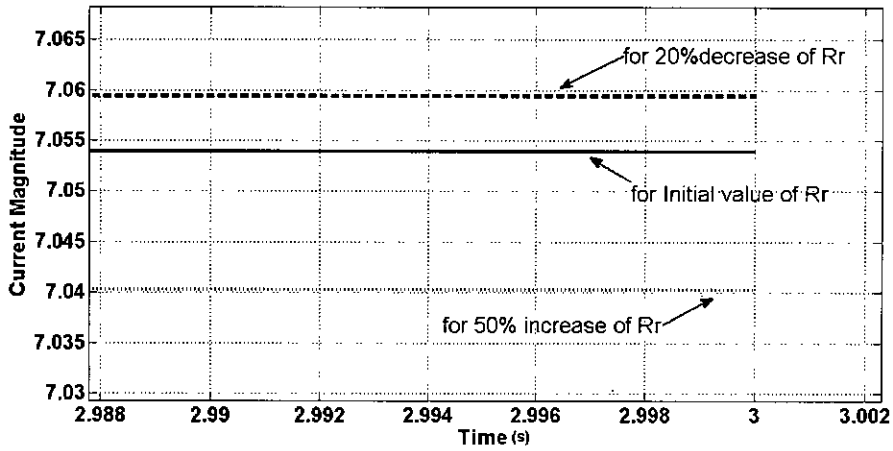


Figure 4.49: The change of current due to change of rotor resistance for a 5hp motor

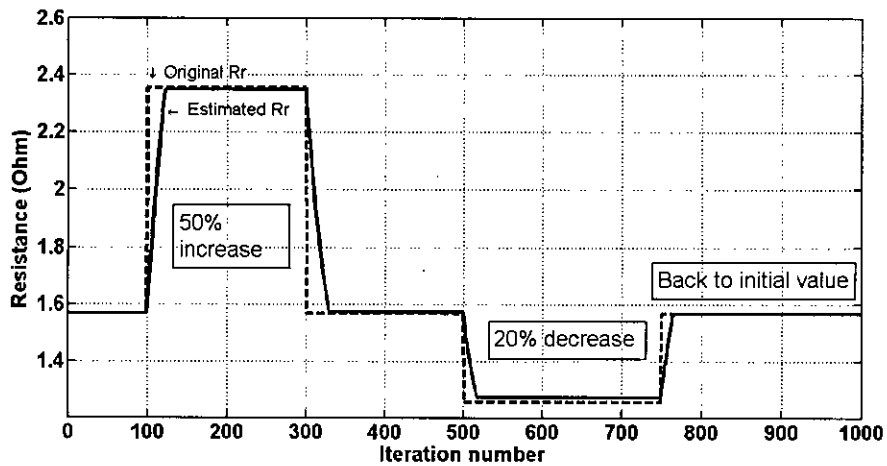


Figure 4.50: The estimated rotor resistance is tracking the change made in the simulation for a 5hp motor



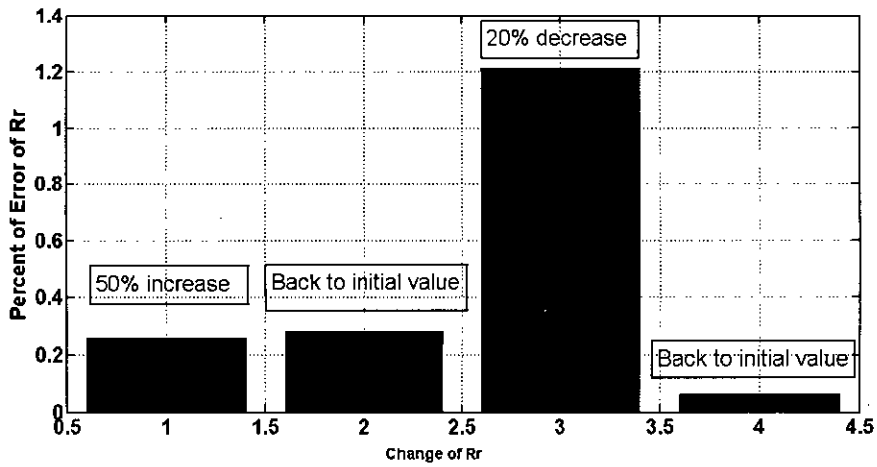


Figure 4.51: The percentage of error while tracking the change made in the simulation for a 5hp motor

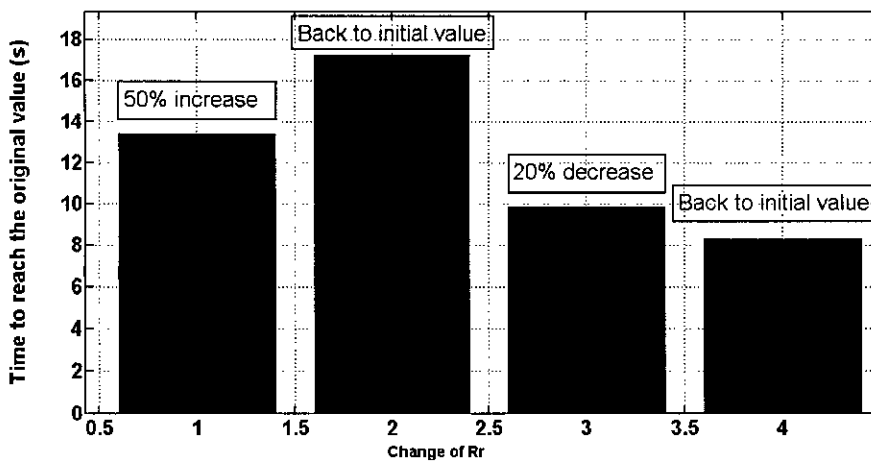


Figure 4.52: The time to reach the original changed value while tracking the change made in the simulation for a 5hp motor

and the parameters were calculated from test data. The parameters of the 3hp and the 5hp motor is taken from [20]. The simulated output of different variables with changing different parameters is presented. Changing the rotor resistance the magnitude of the  $d - q$  current vector is also shown. It is found for each motor that with changing the resistance the current magnitude changes. The error increases if the change in rotor resistance is increases. The adaptive scheme depends on this error. From the simulation it is obvious that the scheme can successfully track the rotor resistance. The percentage of error is quite acceptable. The time to reach the changed value may seem to be high. But it is expected that in practical situation the temperature of the motor will not increase abruptly. So the model should successfully track the practical change in the rotor resistance.

# Chapter 5

## Experimental Results

The experimental results are presented. The results of the adaptation process applied to a one horse power motor is investigated. The test data for an 1hp motor that is used here for experimental validation is presented. The details of the experimental installation, the method to capture the three phase voltages, the three phase currents and data acquisition process is also presented. The MATLAB GUIDE interface and the result from the software is presented.

### 5.1 The Test Data of an 1hp Motor

The no-load and blocked rotor test data is collected for an 1hp motor. From the DC test the resistance of the stator was found as  $13.1\Omega$ . The blocked rotor and no load test data is given in Table 5.1 and Table 5.2.

The calculated parameters from the test data is given in Table 5.3.

### 5.2 Hardware for Voltage Acquisition

The 1hp motor was placed in a board. The three stator winding of the motor were connected in  $Y$  connection. The three phase power was provided from the three phase supply available

Table 5.1: Blocked rotor test data for an 1hp motor

Parameter	Value	Unit
$V_{ph}$	96.4	V
$I_{sc}$	3.06	A
$P_{ph}$	223	W

Table 5.2: No load test data for an 1hp motor

Parameter	Value	Unit
$V_{ph}$	223	V
$I_{ph}$	1.2	A
$P_{ph}$	139	W

Table 5.3: The parameters for an 1hp motor

Parameter	Value	Unit
$R_s$	13.1	$\Omega$
$R_r$	10.71	$\Omega$
$L_{sl}$	32.8	mH
$L_{rl}$	32.8	mH
$L_m$	570	mH

in the Switch-gear and Protection Lab of the Department of Electrical and Electronic Engineering, BUET. The whole installation was placed in the same laboratory. To capture the three phase voltages to the computer the three phase supply needs to be stepped down. Three 220V – 12V, 5A transformers were bought for this purpose. The three transformers were Y connected in the primary side. The neutral of that Y connection was connected to the neutral of the motor Y connection. The output of the three transformers were further stepped down through resistance voltage divider to restrict the voltage provided to the data acquisition card to comply with the input limit of the card. As the maximum input limit of the card channels is 10V. The resistance voltage divider was set to 5 by 1 so that the maximum voltage that may occur across the channels should not go beyond the limit even when an inrush voltage comes at the moment of switching off the motor. The switching transients as captured by the data acquisition card is shown in Figure 5.1

### 5.3 Hardware for Current Acquisition

The value of three phase currents were passed to the data acquisition card through current transformers. Three current transformers of Yokogawa Electric Corporation which were also available in the Switch-gear and Protection Lab. The primary vs secondary turns ratio is 300 by 5. The outputs of the current transformers were shorted by three 0.5 $\Omega$  each. This

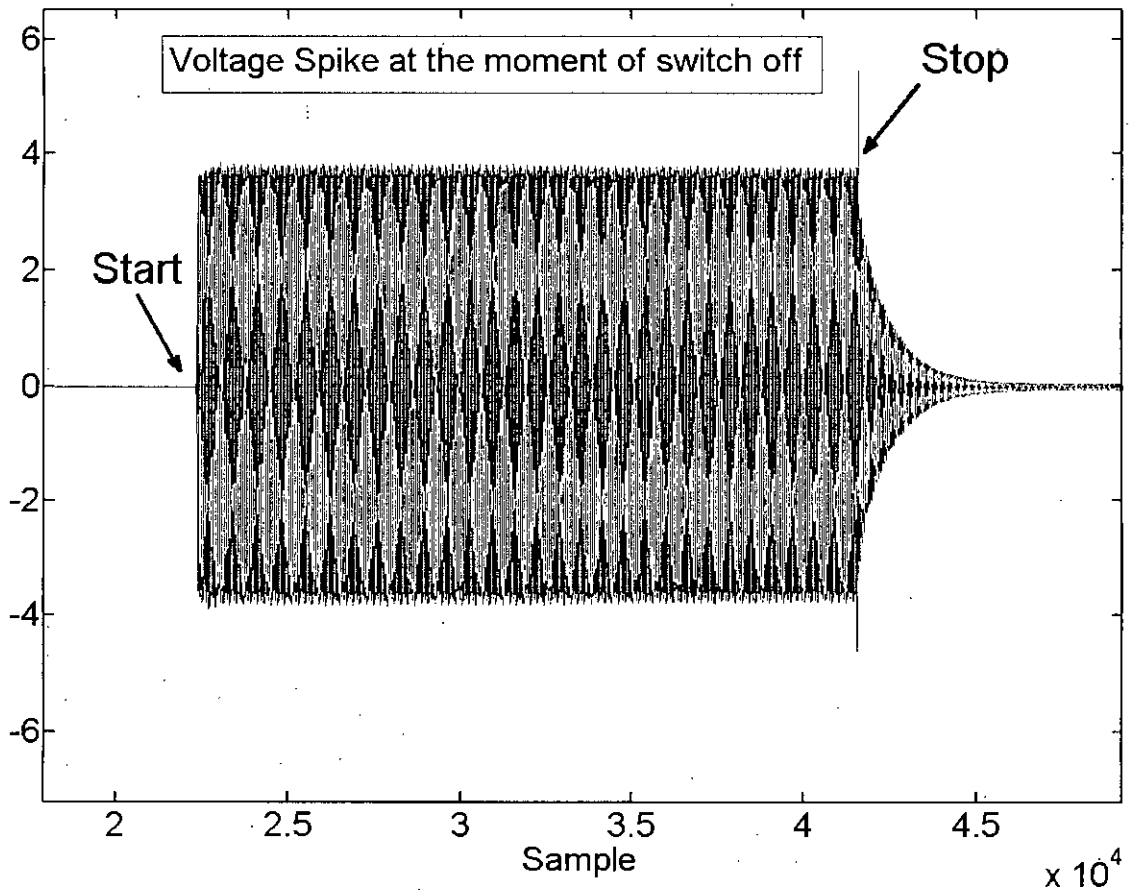


Figure 5.1: The switching inrush in the three phase voltages from the data acquisition card.

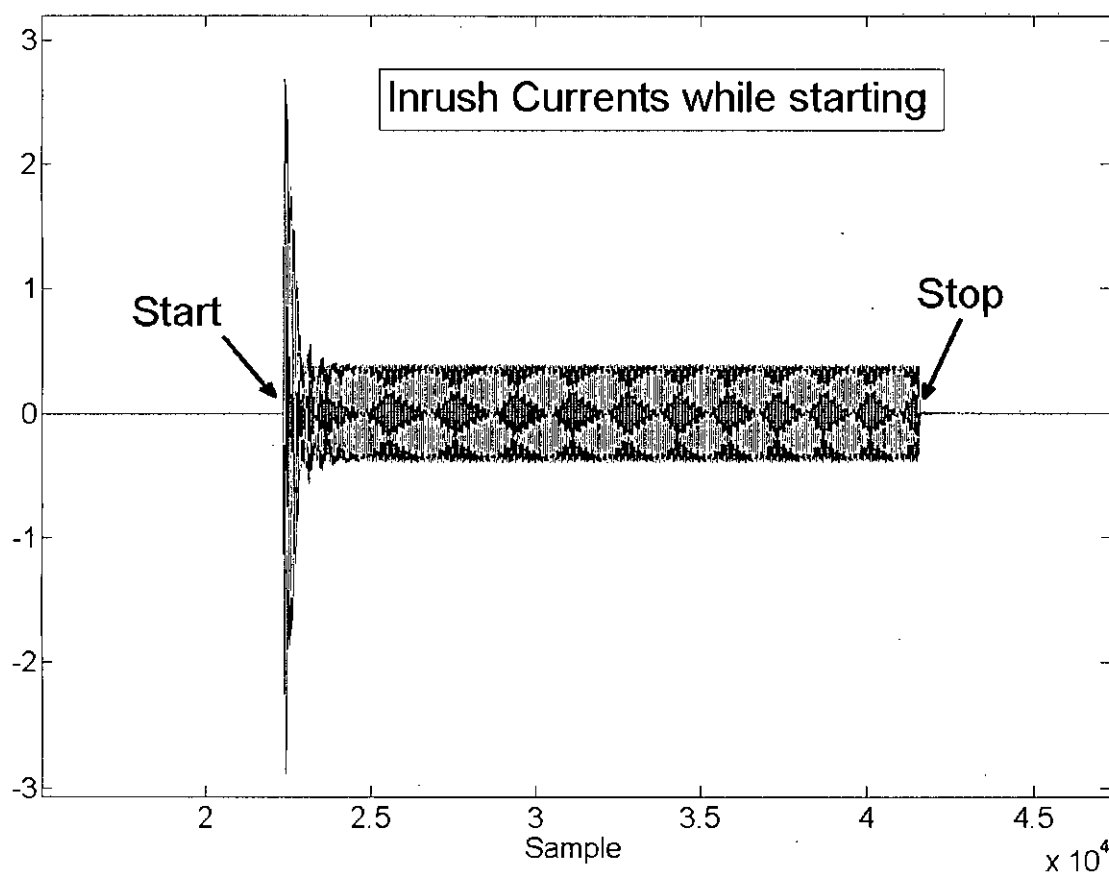


Figure 5.2: The switching inrush in the three phase currents from the data acquisition card.

time also the voltage across the  $0.5\Omega$  is within the limit of the data acquisition card. The inrush current while switching on the motor is higher than the steady state current. The switching transients while switching on the motor is shown in Figure 5.2

## 5.4 The Data Acquisition Card for Capturing Three Phase Voltages and Currents

The data acquisition card used here is PCI-1711L of Advantech Corporation. It has 16 analog input channels. The maximum sampling rate of the card per channel is 100 kilo sample per second. For the hardware in the loop simulation 10 kilo sample per second per channel were used. The three phase voltages and currents sampled to the computer were calibrated. For calibration purpose of the voltages the multiplying factor were calculated by dividing the measured the input voltages to the transformers by a high precision multimeter

106082

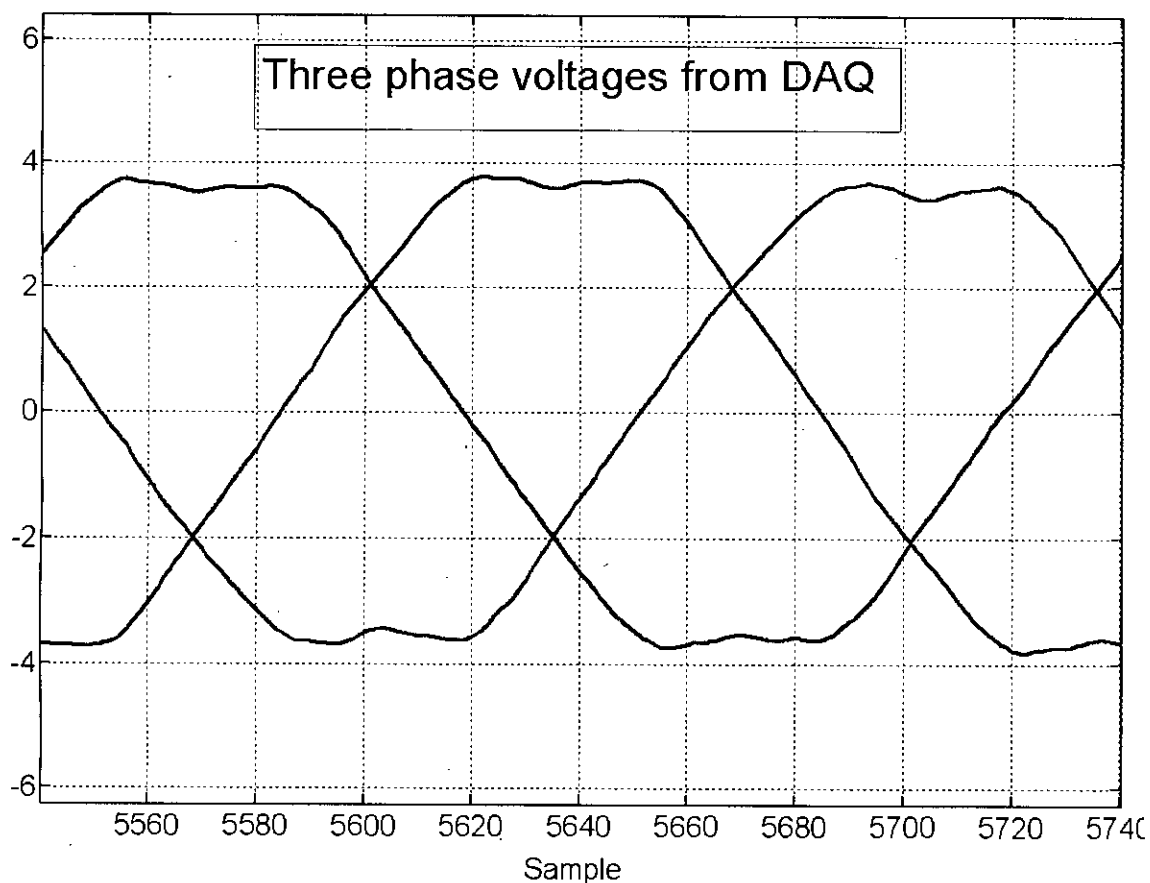


Figure 5.3: The three phase voltages from the data acquisition card.

by the sampled voltages from the data acquisition card.

For the calibration of the currents measured by the data acquisition card the three phase currents were also measured by high precision current meters and the proper multiplying factors were calculated as well.

The captured raw data from the three phase voltages is shown in Figure 5.3.

The captured raw data from the three phase currents is shown in Figure 5.4

The  $d - q$  currents calculated from experimental currents are shown in Figure 5.5

The experimental setup of the whole system is shown in Figure 5.6

## 5.5 The Adaptation Software Made by MATLAB GUIDE

The captured data by the card is fed to the 3 phase to 2 phase converter in the scheme. Then the calculated  $d - q$  current vector magnitude is compared with the output from the adaptive

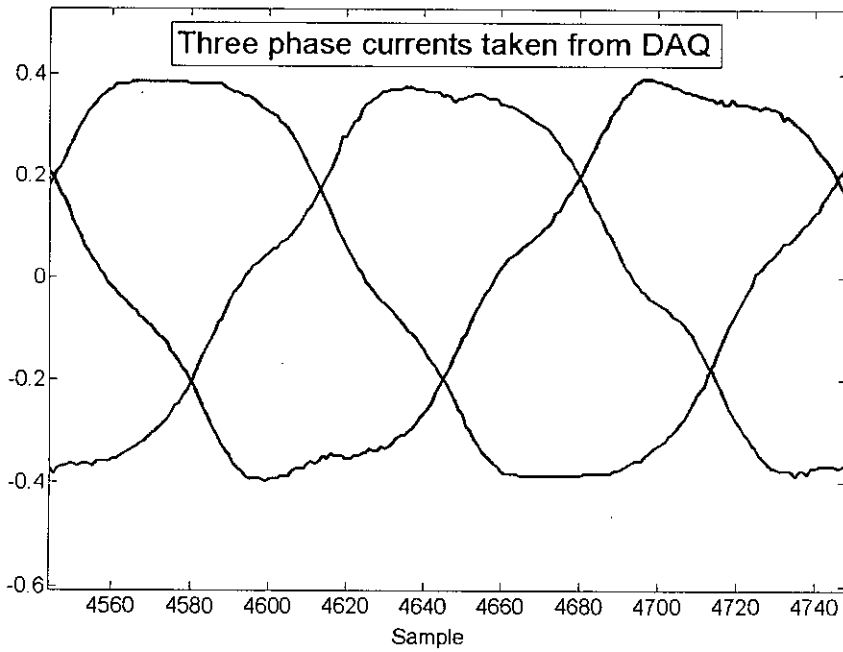


Figure 5.4: The three phase currents from the data acquisition card.

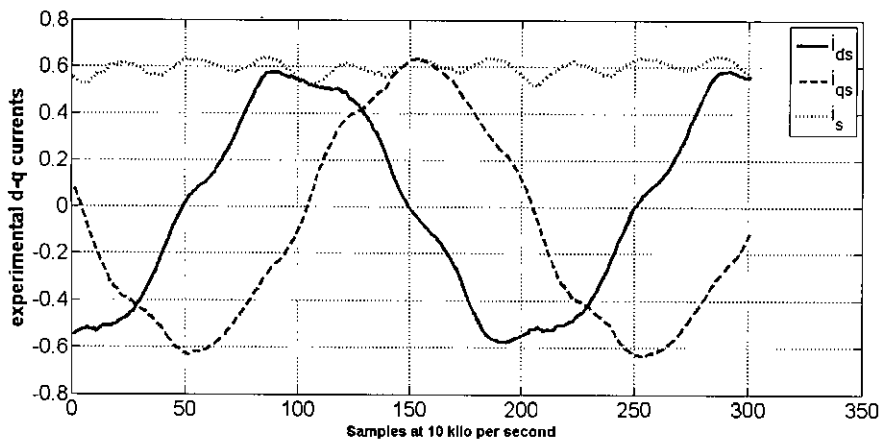


Figure 5.5: The experimentally captured and converted  $d - q$  currents



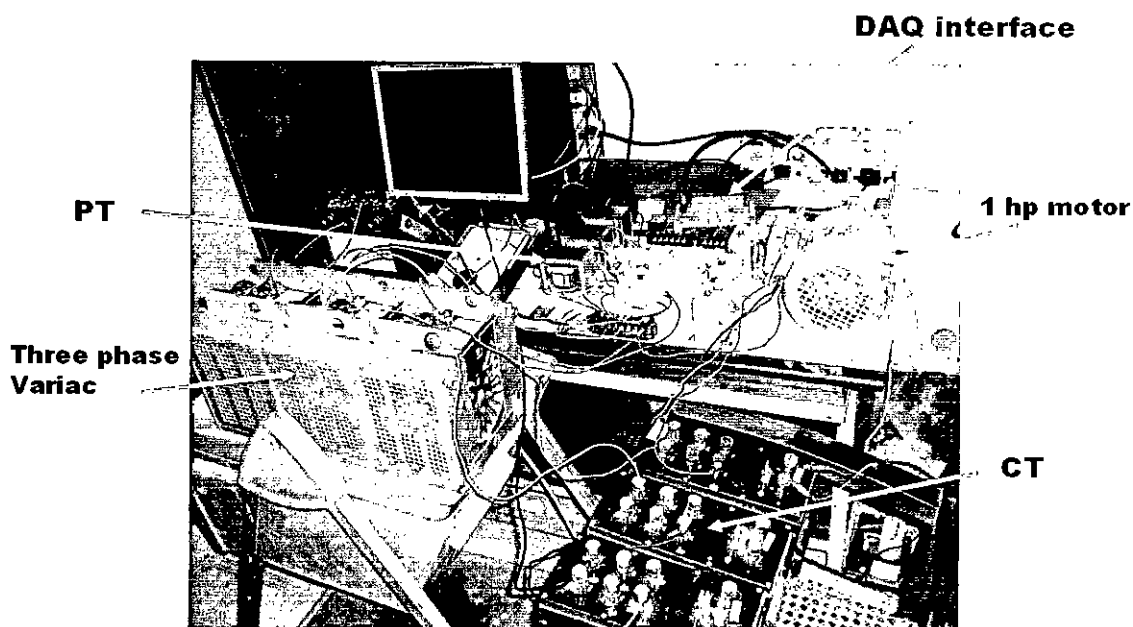


Figure 5.6: The experimental setup of the whole system

model and the error is fed to a PI block to update the rotor resistance as well. A software window was prepared by MATLAB Graphical User Interface Development Environment (GUIDE). There is a start button in the window. By pressing this start button the data acquisition will start and the adaptation m file will start to work. The update in the plot is dynamic. The value of the estimated rotor resistance is also updated in a text box. Two sample of the window while estimating the rotor resistance is shown in Figure 5.7 and 5.8

From the experimental output shown in Figure 5.7 and 5.8 it is obvious that the adaptive model is adapting the rotor resistance. Though it is not verified that whether the estimated output proposed from the Figure had actually reached to the accurate rotor resistance, it is expected that it should at least increase to 30 to 50 percent of its initial parameter extracted from test data. The change should be gradual as the temperature inside the motor increases gradually. So it is proposed that the same model should work successfully to other motors with higher power ratings.

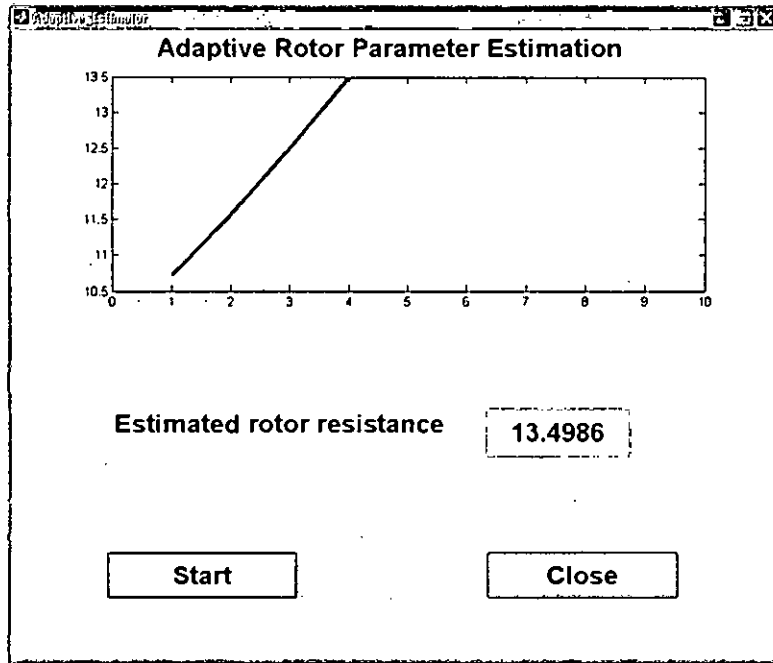


Figure 5.7: The software window showing successful estimation of the rotor resistance

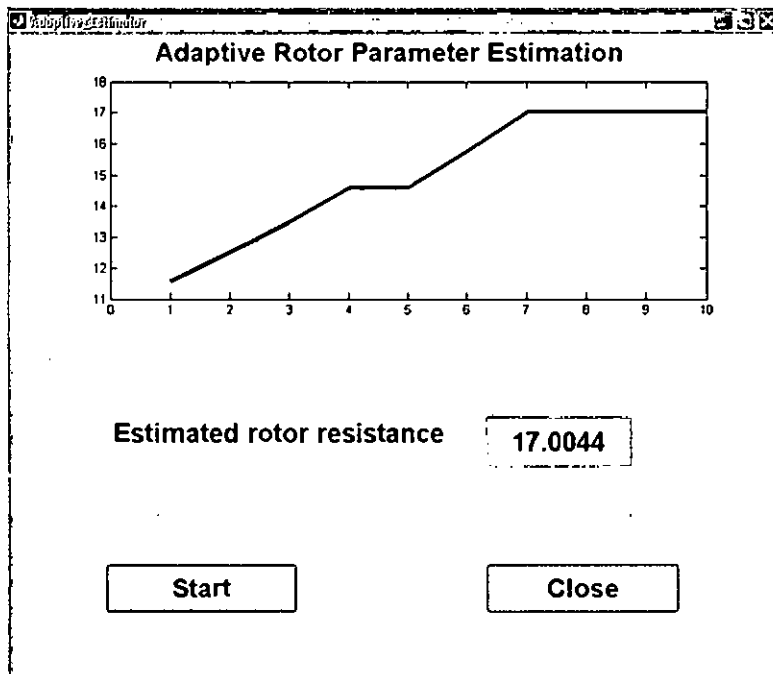


Figure 5.8: The software window showing successful estimation of the rotor resistance

# Chapter 6

## Conclusions and Future Works

### 6.1 Conclusions of the Thesis

This thesis reports the results of a detailed investigation of the application of an adaptive scheme in tracking the rotor resistance for a three phase induction motor drive. The main aim of the project was to track the rotor resistance of an induction motor quickly and accurately, using a sensorless adaptive model. The critical parameter in an induction motor drive is the rotor resistance. The problem of rotor time constant or rotor resistance adaptation in rotor flux oriented vector control of induction motors has been a subject of vigorous research for the last twenty years. The classical and current methods are described in the introduction chapter. This thesis has included a review of the literature on the rotor parameter estimation.

To understand the adaptive scheme a rigorous theory of the motor model is provided. At first the detailed theory of the motor equations in  $abc$  reference frame is included. Then the theory to transform the equations in  $d - q$  arbitrary reference frame, stator reference frame, synchronously rotating reference frame, rotor reference frame is presented.

The adaptive scheme is presented step by step. The estimation time varies according to the threshold value of the error and the proportional constant value. The change of rotor resistance was abrupt in the simulation. But in practical scenario the resistance does not vary abruptly. As the main reason of changing the resistance is temperature, it is expected that the temperature will not increase or decrease abruptly. So in the same way it is expected that the resistance will vary with a certain gradient depending on the reason of change.

The adaptation scheme worked fine in simulation with lower percentage of errors. As the power rating of the motor increases the percentage of errors decreases. In industry

normally the rating is many times higher than the motors so far simulated and analyzed. The resistance of higher rated motors is lower. So the sensitivity of change of resistance with temperature in that case also increases. That is the reason that the performance of the scheme is better for higher rated motors.

However the error threshold value was increased the proportional value was changed as well for hardware in the loop experimental simulation. It was changed for improving the adaptation scheme.

## 6.2 Future Works Proposed

The hardware in the loop adaptive scheme was verified only for an 1hp motor. If it is done for several other higher rated motors then the adaptive scheme can be improved further. Different constants used in the model is selected fixed through rigorous hardware in the loop simulation. These constants should be more precise if the same simulation is done for several other motors.

The model can be further improved if the PI block is replaced by a fuzzy block. For a certain rated motor the input output variables can be fuzzified before using the adaptive scheme. The predetermined block constants then can be used. Through the use of fuzzy block the time to track the change and reliability can be further improved.

The voltage and current sensors used here should have certain percentage of errors. A high performance potential transformer for better sensing the voltages and hall effect current sensors can be used for better sensing the three phase currents. The accuracy of the sensors is also a issue for reliability of the scheme. So sensors with more precision.

Moreover the scheme is for a constant load system. For systems where the load varies a torque feedback loop should be applied to the scheme. In that case it can get a wide range of the application.

## References

- [1] K. Abdel, K. Nabti, and H. Benalla, "A new sml observer implementation for speed sensorless based robust irfoc induction machine drives," *International journal of Electric and Power Engineering*, vol. 2(4), pp. 277–282, 2008.
- [2] D. Marcetic and S. Vukosavic, "Speed-sensorless ac drives with the rotor time constant parameter update," *IEEE Transactions on Industrial Electronics*, vol. 54, pp. 2618 – 2625, Oct. 2007.
- [3] J. Thongam, M. Ouhrouche, F. Haghgoeian, and H. Ezzaidi, "Simultaneous estimation of speed and rotor resistance in sensorless induction motor vector controlled drive," *International Journal of Modelling and Simulation*, vol. 10, pp. 1576–1583, 2007.
- [4] F. Blaschke, "The principle of field orientation as applied to the new transvector closed loop system for rotating field machines," *Siemens Review*, vol. 34, pp. 217–220, May 1972.
- [5] T. Matsuo and T. A. Lipo, "A rotor parameter identification scheme for vector controlled induction motor drives," *IEEE Transactions on Industry Applications*, vol. 21, pp. 624–632, May/June 1985.
- [6] H. A. Toliyat and A. A. G. Hosseiny, "Parameter estimation algorithm using spectral analysis for vector controlled induction motor drives," in *IEEE Interanational Symposium on Industrial Electronics*, pp. 90–95, 1993.
- [7] R. Gabriel and W. Leonard, "Microprocessor control of induction motor," in *International Semiconductor Power Conversion Conference*, pp. 385–396, 1982.

- [8] B. K. Bose and N. R. Patel, "A sensorless stator flux oriented vector control of induction motor using extended kalman filter," in *IEEE IAS Annual Meeting*, pp. 393–400, 1997.
- [9] J. W. Finch, D. J. Atkinson, and P. P. Acarnley, "Full order estimator for induction motor states and parameters," *Proc. Institute of Electrical Engineers, Electric Power Applications*, vol. 145, no. 3, pp. 169–179, 1998.
- [10] H. Kubota, k. Matsuse, and T. Nakano, "Dsp-based speed adaptive flux observer of induction motor," in *IEEE Transactions on Industrial Applications*, pp. 344–348, 1993.
- [11] K. Ohnishi, Y. Ueda, and K. Miyachi, "Model reference adaptive system against rotor resistance variation in induction motor drive," *IEEE Transactions on Industrial Electronics*, vol. IE- 33, pp. 217–223, 1986.
- [12] F. Zidani, M. S. Nait-Said, M. E. H. Benbouzid, D. Diallo, and R. Abdessemed, "A fuzzy rotor resistance updating scheme for an ifoc induction motor drive," *IEEE Power Engineering Review*, pp. 47–50, Nov. 2001.
- [13] E. Bim, "Fuzzy optimization for rotor constant identification of an indirect foc induction motor drive," *IEEE Transactions on Industrial Electronics*, vol. 48, pp. 1293–1295, Dec. 2001.
- [14] M. Ta-Cao and H. Le-Huy, "Rotor resistance estimation using fuzzy logic for high performance induction motor drives," in *IEEE Industrial Electronics Society Annual Meeting*, pp. 303–308, 1998.
- [15] D. Fodor, G. Griva, and F. Profumo, "Compensation of parameters variations in induction motor drives using a neural network," in *IEEE Power Electronics Specialists Conference*, pp. 1307–1311, 1995.
- [16] A. Ba-Razzouk, A. Cheriti, and G. Olivier, "Artificial neural networks rotor time constant adaptation in indirect field oriented control drives," in *IEEE Power Electronics Specialists Conference*, pp. 701–707, 1996.

- [17] S. Mayaleh and N. Bayinder, "On-line estimation of rotor time constant of an induction motor using recurrent neural networks," in *IEEE Workshop Computers in Power Electronics*, pp. 219–223, 1998.
- [18] P. C. Krause, *Analysis of Electric Machinery*. McGraw-Hill Book Company, 1986.
- [19] B. K. Bose, *Modern Power Electronics and AC Drives*. Pearson Education, 2004.
- [20] T. Phumiphak and C. Chat-uthai, "Estimation of induction motor parameters based on field test coupled with genetic algorithm," in *IEEE International Conference on Power System Technology*, 2002.

